

Author Manuscript

This is the author manuscript accepted for publication and has undergone full peer review but has not been through the copyediting, typesetting, pagination and proofreading process, which may lead to differences between this version and the [Version of Record](#). Please cite this article as [doi: 10.1111/1365-2435.13618](https://doi.org/10.1111/1365-2435.13618)

This article is protected by copyright. All rights reserved

1 **Nutrient limitation, bioenergetics, and stoichiometry: a new model to predict elemental**
2 **fluxes mediated by fishes**

3 Nina M. D. Schiettekatte^{1,2,*}, Diego R. Barneche^{3,4,5}, Sébastien Villéger⁶, Jacob E. Allgeier⁷,
4 Deron E. Burkepile^{8,9}, Simon J. Brandl¹⁰, Jordan M. Casey^{1,2}, Alexandre Mercière^{1,2}, Kat-
5 rina S. Munsterman⁷, Fabien Morat², Valeriano Parravicini^{1,2}

6 ¹ PSL Université Paris: EPHE-UPVD-CNRS, USR 3278 CRIOBE, Université de Perpignan, 66860 Perpignan,
7 France

8 ² Laboratoire d'Excellence "CORAIL," Perpignan, France

9 ³ Australian Institute of Marine Science, Crawley, WA 6009, Australia

10 ⁴ Oceans Institute, The University of Western Australia, 35 Stirling Hwy, Crawley, WA, 6009, Australia

11 ⁵ College of Life and Environmental Sciences, University of Exeter, Penryn TR10 9FE, UK

12 ⁶ Université Montpellier, CNRS, IFREMER, IRD, 34 095 Montpellier, France

13 ⁷ Department of Ecology and Evolutionary Biology, University of Michigan, Ann Arbor, Michigan 48109, USA

14 ⁸ Department of Ecology, Evolution, and Marine Biology, University of California, Santa Barbara, Santa Bar-
15 bara, CA, United States

16 ⁹ Marine Science Institute, University of California, Santa Barbara, Santa Barbara, CA, United States

17 ¹⁰ Department of Biological Sciences, Simon Fraser University, Burnaby, BC V5A 1S6, Canada

18 **Correspondence to:** N.M.D.S.; Email: nina.schiettekatte@gmail.com

19 **Running title:** Modelling elemental fluxes in fishes

20 **Key-words:** nitrogen, phosphorus, bioenergetics, nutrient cycling, fish, stoichiometry, inges-
21 tion, excretion, nutrient limitation

22 **Acknowledgements**

23 We thank the staff at CRIOBE, Moorea for field support. We would also like to thank Benoit
24 Espiau, Calvin Quigley, Kaitlyn Landfield and Tommy Norin for their help in the field, and
25 Guillemette de Sinéty and Jérémy Wicquart for their contribution to otolith analysis. This
26 work was supported by the BNP Paribas Foundation as a part of the ReefServices project, the
27 Agence National de la Recherche (REEFLUX, ANR-17-CE32-0006) and the U.S. National
28 Science Foundation (OCE-1547952). Finally, we thank two anonymous reviewers, whose
29 comments substantially improved this manuscript.

30 **Author contributions**

31 NMDS conceived the idea and NMDS, VP, DRB and SV designed methodology; NMDS,
32 JMC, SJB, AM, FM, VP, KSM, JEA and DEB collected the data; NMDS analysed the data
33 and led the writing of the manuscript. All authors contributed significantly to the drafts and
34 approved the final version for publication.

Author Manuscript

1 Nutrient limitation, bioenergetics, and stoichiometry: a new model to predict elemental 2 fluxes mediated by fishes

3 Abstract

4 1. Energy flow and nutrient cycling dictate the functional role of organisms in ecosystems.

5 Fishes are key vectors of carbon (C), nitrogen (N), and phosphorus (P) in aquatic systems, and
6 the quantification of elemental fluxes is often achieved by coupling bioenergetics and stoi-
7 chiometry. While nutrient limitation has been accounted for in several stoichiometric models,
8 there is no current implementation that permits its incorporation into a bioenergetics approach
9 to predict consumption rates. This may lead to biased estimates of elemental fluxes.

10 2. Here, we introduce a theoretical framework that combines stoichiometry and bioenergetics
11 with explicit consideration of elemental limitations. We examine varying elemental limitations
12 across different trophic groups and life stages through a case study of three trophically-distinct
13 reef fishes. Further, we empirically validate our model using an independent database of mea-
14 sured excretion rates.

15 3. Our model adequately predicts elemental fluxes in the examined species and reveals
16 species- and size-specific limitations of C, N, and P. In line with theoretical predictions, we
17 demonstrate that the herbivore *Zebrasoma scopas* is limited by N and P, and all three fish
18 species are limited by P in early life stages. Further, we show that failing to account for
19 nutrient limitation can result in a greater than two-fold underestimation of ingestion rates,
20 which leads to severely biased excretion rates.

21 4. Our model improved predictions of ingestion, excretion, and egestion rates across all life
22 stages, especially for fishes with diets low in N and/or P. Due to its broad applicability, its
23 reliance on many parameters that are well defined and widely accessible, and its straightfor-
24 ward implementation via the accompanying R-package `fishflux`, our model provides a user-
25 friendly path toward a better understanding of ecosystem-wide nutrient cycling in the aquatic
26 biome.

27 **Introduction**

28 Internal biological processes of consumer species, such as growth, respiration, and excretion
29 are important drivers of ecosystem-scale biogeochemical cycles (Welti et al., 2017). To sur-
30 vive, individuals need to gather resources from the environment and, in doing so, transfer en-
31 ergy and nutrients within and across ecosystems (Brown, Gillooly, Allen, Savage, & West,
32 2004; Mackenzie, Ver, Sabine, Lane, & Lerman, 1993). Therefore, the quantification of en-
33 ergy and nutrient fluxes in ecosystems is affected by our ability to understand how energy and
34 materials are utilized and transformed at the individual level (Allgeier, Yeager, & Layman,
35 2013; Kitchell et al., 1974; Sterner & Elser, 2002).

36 In many aquatic ecosystems, fishes account for most of the heterotrophic biomass (Odum &
37 Odum, 1955; Vanni, 2002) and contribute substantially to the storage and flux of carbon (C),
38 nitrogen (N), and phosphorus P (Allgeier, Layman, Mumby, & Rosemond, 2014; Barneche
39 et al., 2014; Burkepile et al., 2013; McIntyre et al., 2008; Vanni, 2002). Storage is primarily
40 dictated by food that is assimilated and allocated to growth, which ultimately underpins crit-
41 ical ecosystem services (e.g., finfish fisheries). Fluxes are derived from assimilated (respired
42 carbon and excreted nutrients) and non-assimilated food (egested organic waste) (Schreck &
43 Moyle, 1990), and they can have important effects on ecosystem processes, such as primary
44 production (Allgeier et al., 2013; Capps & Flecker, 2013; McIntyre et al., 2008). Disentan-
45 gling how fishes partition ingested elements into biomass and waste products is therefore key
46 to linking individual-level physiology to ecosystem-level processes, which are of inherent
47 human interest (Anderson, Hessen, Elser, & Urabe, 2005; Barneche & Allen, 2018; Hessen,
48 Ågren, Anderson, Elser, & De Ruiter, 2004; Hou et al., 2008).

49 Ecological stoichiometry provides a theoretical framework to understand how consumers par-
50 tition C, N, and P (Sterner & Elser 2002). On the basis of the conservation of mass, the mate-
51 rial ingested by consumers equals the sum of biomass accumulation and waste products such
52 as respired carbon, excreted nutrients, and egested organic material. Furthermore, stoichio-
53 metric theory predicts that the ratio of recycled elements depends on the elemental composi-
54 tion of the consumer body, diet, and the gross growth efficiency of the limiting element (Frost

55 et al., 2006; Sterner, 1990). Thus, given known consumption rates, stoichiometric mass bal-
56 ance models allow for the prediction of fish excretion rates (Kraft, 1992; Schindler & Eby,
57 1997). Consumption rates can be approximated using empirical relationships with body mass
58 and temperature (e.g., Elliott & Persson, 1978; El-Sabaawi, Warbanski, Rudman, Hovel, &
59 Matthews, 2016), but these estimates are highly species-specific, require extensive lab experi-
60 ments, and may not reflect fish consumption rates in the wild.

61 Alternatively, consumption rates can be estimated using bioenergetic models. In fact, there is
62 a rich history of bioenergetic modelling approaches to estimate energy allocation in fishes un-
63 der the assumption that they are limited by energy (C) (e.g., the “Wisconsin model”, Kitchell
64 et al. (1974); Hanson, Johnson, Schindler, & Kitchell (1997) and the “Dynamic Energy Bud-
65 get model”, Kooijman (2010)). Combined with elemental stoichiometry, bioenergetic models
66 therefore provide a conceptual basis to predict how fishes partition energy and nutrients into
67 growth, metabolism, and waste (Deslauriers, Chipps, Breck, Rice, & Madenjian, 2017; Kraft,
68 1992; Schindler & Eby, 1997; Schreck & Moyle, 1990). This approach has been widely used
69 to estimate consumption rates, given known growth rates in wild fish populations (especially
70 via the Fish Bioenergetics software; Deslauriers et al., 2017). Nutrient cycling predictions are
71 then made by combining modeled ingestion rates based on energetic needs, assimilation ef-
72 ficiencies, and nutrient stoichiometry of both a fish’s body and diet (Anderson et al., 2005;
73 Kraft, 1992; Schindler & Eby, 1997).

74 Although useful and successfully implemented (Deslauriers et al., 2017), this approach is
75 limited in its application to fishes that are limited by C. This can be the case, especially for
76 trophic groups that feed on nutrient-rich prey (e.g., Schindler & Eby, 1997); yet, many fish
77 species in low trophic levels may be limited by N or P because their diets contain lower nu-
78 trient levels than their body tissues (McIntyre et al., 2008; Schindler & Eby, 1997). Thus, ap-
79 plying the traditional approach of combining stoichiometry and bioenergetics (Kraft, 1992) to
80 fish species that are limited by N or P normally results in biologically implausible predictions
81 of excretion rates. Indeed, there is mounting evidence that fishes can be limited by nutrients,
82 rather than energy (Benstead et al., 2014; El-Sabaawi et al., 2016; Hood, Vanni, & Flecker,
83 2005; Moody, Lujan, Roach, & Winemiller, 2019). While, negative predicted excretion rates

84 can provide evidence for nutrient limitation (e.g., Hood et al., 2005), they do not aid our un-
85 derstanding and prediction of realistic elemental fluxes in communities where nutrient-limited
86 species are prevalent. Thus, although many stoichiometric models take into account nutrient
87 limitation (e.g., Sterner, 1990; El-Sabaawi et al., 2016; Guariento, Luttbeg, Carneiro, & Cal-
88 iman, 2018; Moody et al., 2018, 2019), there is presently no solution for integrating nutrient
89 limitation into bioenergetic models that quantify consumption rates. As fishes in low trophic
90 levels often account for a significant proportion of biomass (e.g., Graham et al., 2017) and
91 represent important vectors of nutrients, a new approach is needed to accurately predict ele-
92 mental fluxes in the absence of known consumption rates.

93 Here, we present a theoretical framework (and a companion R package for its implementa-
94 tion: `fishflux`) to predict elemental fluxes in fishes that combines bioenergetics and eco-
95 logical stoichiometry while directly accounting for N and P limitation, alongside C limita-
96 tion. The proposed model framework predicts ingestion rates based on the needs of a fish at
97 a certain size for all three elements and a known growth rate. We test our framework via a
98 case study of three trophically-distinct coral reef fish species: the herbivore *Zebrasoma scopas*
99 (family Acanthuridae), the omnivore *Balistapus undulatus* (family Balistidae), and the carni-
100 vore *Epinephelus merra* (family Serranidae). We also validate our model against independent
101 empirical excretion estimates for our three fish species. Furthermore, we test whether fishes
102 in different trophic levels and life stages are limited by different elements and hypothesize
103 that fishes at low trophic levels are limited by N or P rather than C. Finally, we posit that, by
104 building on existing approaches, our framework considerably improves the prediction of key
105 processes such as ingestion and excretion in the case of strong nutrient limitation, as compared
106 to models that only consider C-limitation.

107 **Materials and Methods**

108 **1. Theoretical framework**

109 Carbon, nitrogen, and phosphorus (CNP, expressed in grams) are the three chemical elements
110 considered in our model. The approach applies a mass-balance framework based on ecolog-
111 ical stoichiometry and the metabolic theory of ecology (Brown et al., 2004; Sterner & Elser,
112 2002). Further, the approach relies on the growth trajectory of natural fish populations. The
113 proposed model has four main steps (Fig. 1): (1) The minimal required ingestion or minimal
114 supply rate of CNP is defined as the sum of CNP needed for a given growth increment and
115 minimal inorganic flux (i.e., the minimal requirements of CNP needed for metabolism and the
116 maintenance of the body stoichiometry). In this step, we also consider assimilation efficiency,
117 which is defined as the capacity of an organism to assimilate C, N or P (input parameters of
118 the model). (2) Ingestion is estimated based on the limiting element that is defined by the im-
119 balance between the CNP composition of the minimal supply rate and that of the diet. (3) The
120 egestion rate is then quantified according to the ingestion rate and the assimilation efficien-
121 cies of each element. (4) The residual CNP are allocated toward the total inorganic flux of
122 CNP (i.e., the waste inorganic CNP that is produced from physiological transformation). For
123 the sake of comparison with existing literature, we note that the inorganic flux of C is gener-
124 ally called total metabolic rate, whereas the inorganic fluxes of N and P are called excretion
125 rates. Materials that are not assimilated are egested as organic waste. An overview of all main
126 variables predicted by the model and input parameters that need to be specified by the user is
127 given in Table 1, while other parameters mentioned in the text are fixed in the model. In the
128 following sections, we detail each component of the model.

129 *1.1. Minimal supply rate*

130 The first step of the model is an estimate of the minimal supply rate of elements (C, N and P)
131 required per day for a given growth increment in an individual of a given size. The required
132 CNP is the sum of the elements needed for body mass growth and overhead metabolic and
133 maintenance costs (i.e., minimal inorganic flux). The minimal supply rate S_k (g d^{-1}) of the

134 element $k = \{C, N, P\}$ can therefore be estimated as

$$S_k = \frac{(G_k + F_{0k})}{a_k}, \quad (1)$$

135 where G_k , F_{0k} and a_k are element-specific growth rate (g d^{-1}), minimal inorganic flux (g d^{-1}),
136 and assimilation efficiency (%), respectively.

137 1.1.1. Growth

138 The aim of our model is to predict elemental fluxes of fishes in their natural environment.

139 Therefore, we use growth rates that can be calculated from otolith analysis. In our model, we
140 thus assume that there is enough food available to fulfill the observed growth pattern. We fur-
141 ther use the von Bertalanffy growth curve (VBGC) to describe the growth trajectory (Berta-
142 lanffy, 1957). Empirically, the VBGC is favorable because its parameters are statistically sim-
143 ple to obtain, easy to interpret, and are available for a large number of species (Morais & Bell-
144 wood, 2018). Body length, l_t (cm in total length, i.e., T.L.), at age t (yr) is

$$l_t = l_\infty \left(1 - e^{-\kappa(t-t_0)}\right), \quad (2)$$

145 where t_0 is age at settlement, l_∞ is the asymptotic adult length (i.e., length when growth rate
146 is 0), and κ is a growth rate parameter (yr^{-1}) (Bertalanffy, 1957). With this equation, we can
147 quantify the age of a fish of a certain size. Then, by adding one day to that age, we can also
148 approximate the amount a fish will grow in one day. Using length-weight relationships and
149 wet-to-dry mass conversion constants from the literature and FishBase (Froese & Pauly,
150 2018), we can finally calculate total growth rate (i.e., G) expressed in dry mass (g d^{-1}). Using
151 element-specific body content percentages, Q_k , we calculate element-specific growth as:

$$G_k = \frac{Q_k}{100} G. \quad (3)$$

152 1.1.2 Minimal inorganic flux

153 Traditionally, the field metabolic rate, F_{0C} , has been studied more intensively than minimal

154 excretion rates for N and P, F_{0N} , and F_{0P} . As a consequence, we currently have a better under-
 155 standing of how assimilated carbon is partitioned into body mass growth (G_C) and metabolic
 156 overhead costs (F_{0C}). For instance, we know that F_{0C} predictably scales with individual wet
 157 body mass, m_w (g) (Hou et al., 2008):

$$\begin{aligned}
 F_{0C} &= \theta F_{0Cr} = \\
 &\theta (F_{0Cz} m_w + F_{0Cs}) = \\
 &\theta (f_0 m_w^{\alpha-1} m_w + \phi G),
 \end{aligned} \tag{4}$$

158 where F_{0Cr} is the resting metabolic rate (g C d⁻¹), F_{0Cz} is the mass-specific turnover rate (g C
 159 g⁻¹ d⁻¹), F_{0Cs} is the rate of carbon spent in body mass growth, and f_0 is a metabolic normal-
 160 ization constant that is independent of body mass (g C g^{- α} d⁻¹) and varies among fish taxa,
 161 environmental temperature, and trophic level (Barneche & Allen, 2018). α is a dimensionless
 162 mass-scaling exponent (generally between 0.5 and 1), $m_{w\infty}$ is the asymptotic mass of an in-
 163 dividual, and ϕ is the energy expended to produce one unit of body mass (g C g⁻¹; hereafter
 164 the ‘‘cost of growth’’). In equation 4, F_{0C} is defined as the sum of the resting metabolic rate,
 165 F_{0Cr} , and the active rate that sustains locomotion, feeding, and other activities. We assume
 166 that $F_{0C} = \theta F_{0Cr}$ in the expression above, where θ is a dimensionless parameter referred to as
 167 ‘activity scope’, which is constrained to be greater than 1 and less than the ratio between max-
 168 imum metabolic rate and resting metabolic rate (Barneche & Allen, 2018; Hou et al., 2008).
 169 The cost of growth, ϕ , varies substantially among fishes, and it may increase with environ-
 170 mental temperature, v , trophic level, h , and aspect ratio of caudal fin, r (a proxy for activity
 171 level) (Froese & Pauly, 2018). Following Barneche & Allen (2018), the cost of growth can be
 172 calculated as

$$\ln \phi = \beta_0 + \beta_v v + \beta_h \ln h + \beta_r \ln(r + 1), \tag{5}$$

173 where β_0 is a constant, β_v , β_h , and β_r are respectively the model slopes for v , h , and r . We note
 174 that h and r are two ecological variables that can be retrieved from FishBase (Froese & Pauly,
 175 2018). For the purposes of our bioenergetic model, we use average, across-species estimates
 176 for β_0 , β_v , β_h , and β_r published in Barneche & Allen (2018).

177 Aside from inorganic fluxes of C, N and P will also be released at a minimal rate, even when
 178 they are limiting (Anderson et al., 2005; Sterner & Elser, 2002). The minimal inorganic flux
 179 of N and P can be experimentally measured as minimal excretion rates during starvation
 180 (Mayor et al., 2011). We can thus explicitly incorporate N and P turnover rates to estimate
 181 minimal inorganic flux of N and P (Anderson et al., 2005).

$$F_{0N} = F_{0Nz} \frac{Q_N}{100} m_d, \text{ and} \quad (6)$$

182

$$F_{0P} = F_{0Pz} \frac{Q_P}{100} m_d, \quad (7)$$

183 where F_{0Nz} and F_{0Pz} are nutrient-specific dry mass-specific turnover rates for N ($\text{g N g}^{-1} \text{d}^{-1}$)
 184 and P ($\text{g P g}^{-1} \text{d}^{-1}$), respectively, and m_d is the dry mass of the fish (g). Equations 6 and 7 as-
 185 sume that F_{0Nz} and F_{0Pz} remain constant during ontogeny.

186 1.2. Ingestion

187 In our model, the quantification of ingestion rate is a two-step process. First, we define the
 188 minimal required ingestion of CNP by summing element-specific minimal supply rates S_k .
 189 Second, we approximate the actual ingestion rates by using ecological stoichiometric theory
 190 (Sterner & Elser, 2002). With known elemental stoichiometry of the diet (D_C , D_N , D_P) we can
 191 determine the limiting element as follows:

$$\text{limiting element} = \left\{ \begin{array}{l} C, \quad \text{if } \frac{S_C}{S_N} > \frac{D_C}{D_N} \text{ and } \frac{S_C}{S_P} > \frac{D_C}{D_P} \\ N, \quad \text{if } \frac{S_N}{S_P} > \frac{D_N}{D_P} \text{ and } \frac{S_C}{S_N} < \frac{D_C}{D_N} \\ P, \quad \text{otherwise} \end{array} \right\} \quad (8)$$

192 The actual ingestion rate is then approximated according to the limiting element, following
193 Liebig's minimum law. To do so, we assume fishes have enough food available to meet their
194 minimal needs (S_k). For example, if P is limiting, element-specific ingestion rates, I_k , (g d^{-1})
195 are

$$I_P = S_P, \quad (9)$$

$$I_N = I_P \frac{D_N}{D_P}, \quad (10)$$

$$I_C = I_P \frac{D_C}{D_P}, \quad (11)$$

198 where D_k represents element-specific body content percentage of dietary items. Once inges-
199 tion rate is estimated, the partitioning of the ingested matter into various pathways (i.e., eges-
200 tion, excretion and respiration) can be defined.

201 1.3. Egestion or organic waste production

202 The rate of organic waste production or egestion rate, W_k (g d^{-1}) can be computed using the in-
203 gestion rate of each element and element-specific assimilation efficiencies (Schreck & Moyle,
204 1990):

$$W_k = (1 - a_k)I_k. \quad (12)$$

205 1.4. Total inorganic flux

206 The rate of total inorganic waste production or flux (i.e., total respiration and excretion) equals
207 the ingestion rate minus body mass growth rate and egestion rate for each element (Schreck
208 & Moyle, 1990; Sterner & Elser, 2002). If an element is limiting, the individual is likely to
209 consume other elements in excess in order to meet the target for that limiting element. In
210 such cases, it is often assumed that the exceeding "residual" element will be subject to post-
211 absorptive release via inorganic waste production (i.e., residual flux F_{rk}) to maintain body

212 homeostasis (Anderson et al., 2005). When N or P are limiting, for example, a certain residual
213 amount of C, F_{rC} remains unutilised. However, if C is limiting instead of N or P, excretion
214 rates F_N and F_P will increase by an overhead residual flux F_{rk} . In the example of C limitation,
215 the residual flux F_{rC} would equal zero. We can thus quantify the total inorganic flux as fol-
216 lows:

$$F_k = F_{0k} + F_{rk}, \quad (13)$$

217 where

$$F_{rk} = I_k - G_k - F_{0k} - W_k. \quad (14)$$

218 2. Application

219 We validate our modelling approach using data from three reef fish species: the herbivore *Ze-*
220 *brasoma scopas* (family Acanthuridae), the omnivore *Balistapus undulatus* (family Balisti-
221 dae), and the carnivore *Epinephelus merra* (family Serranidae). All parameters were quanti-
222 fied using empirical data augmented with information from the literature when needed (see
223 supplementary methods, Appendix S1). An overview of all parameter estimates is provided in
224 Appendix S2, Table 1.

225 We ran the model using R (R Core Team, 2019) and Stan (Stan Development Team, 2018).
226 For an easy application of the presented framework, we developed the R package `fishflux`,
227 which provides a set of user-friendly functions to simulate the model, extract the output vari-
228 ables, and visualize the results (see Appendix S1). Parameter means and standard deviations
229 are provided, and a Monte Carlo method is applied to randomly draw each parameter assum-
230 ing normal distributions in each iteration. To account for co-variances among parameters, we
231 used the Stan function `multi_normal_rng()`, which samples each parameter under consider-
232 ation of the co-variance matrix. We included co-variances for body stoichiometry (Q_k), diet
233 stoichiometry (D_k), length-weight parameters (ϵ and b), and metabolic parameters (α and
234 f_0). These parameters were sampled from their log-transformed multinormal distribution then

235 back-transformed to natural scale. All other parameters were sampled from truncated normal
236 distributions, where the lower and upper bounds are the possible ranges of each respective
237 parameter. For our case study, we used 5,000 iterations. If the standard deviation of a given
238 parameter is unknown (e.g., r , reported on FishBase), the function automatically fills in the
239 standard deviation with a very low value of 10^{-9} in order to keep the respective parameter ap-
240 proximately constant at each iteration of the simulation.

241 To compare the predictions of ingestion and excretion rates of our model framework with the
242 case where only C-limitation is considered, we simulated ingestion and excretion rates, based
243 only on the minimal supply rate of C, thus where I_c equals S_c . Excretion rates or total inor-
244 ganic flux rates of N and P are then defined as follows:

$$F_N = S_C \frac{D_N}{D_C} - G_N - W_N, \quad (15)$$

245

$$F_P = S_C \frac{D_P}{D_C} - G_P - W_P. \quad (16)$$

246 We compared the predicted excretion rates for N and P with our own independent database
247 of experimental excretion rates. We collected individual fish using barrier nets, dip nets, cast
248 nets, traps, clove oil, and hook and line across different reef habitats around Moorea, French
249 Polynesia during austral winter of 2016 and 2017 ($n = 128$). We aimed to collect individuals
250 across the size spectrum present in each species. We immediately transported individuals back
251 to shore in an aerated cooler for excretion experiments (see Appendix S1). Excretion rates
252 were measured within a maximum of 3 hours after capture. The capture and handling of fishes
253 for this project were approved in a protocol from the University of California Santa Barbara's
254 Institutional Animal Care and Use Committee (IACUC #915 2016-2019).

255 Finally, to illustrate the effect of diet stoichiometry, we simulated the model with varying % of
256 N and P. For this simulation, we used the parameters of *Z. scopas* and ran the simulation for
257 an individual of 10cm. We kept D_C constant at 20%. The values of D_N and D_P varied around
258 the elemental ratio of S_k . We used color palettes from the R package fishualize (Schiettekatte,
259 Brandl, & Casey, 2019).

260 Results

261 The application of the developed modeling framework reveals distinct elemental limitations
262 across the three species at different lengths (Fig. 2). *Z. scopas* is limited by either N or P over
263 its full size range, with P being the limiting element early in its ontogeny and N becoming
264 the limiting element after reaching approximately 7 cm TL. Although *B. undulatus* and *E.*
265 *merra* are also limited by P at an early life stage, they are predominantly limited by C upon
266 maturation.

267 Our approach demonstrates that defining the limiting element can be critical to predict a
268 species' ingestion rate, which affects all downstream calculations in the model (e.g., excretion
269 rates of N and P) compared to models only considering C limitation (Fig. 3). Specifically,
270 assuming C limitation in *Z. scopas* results in a severe underestimation of ingestion and
271 excretion rates (Fig. 3, A, B and C). In the omnivore *B. undulatus* and the carnivore *E.*
272 *merra*, the limiting element has less influence on ingestion rates. Still, without incorporation
273 of P limitation, model predictions may result in negative excretion rates of P for growing
274 individuals of *B. undulatus* and *E. merra*. In the case of *E. merra*, C-only models predict
275 negative P excretion rates for more than half of the simulations under a total length of 10 cm
276 (Fig.3, I). Thus, our framework reveals that nutrient limitations and their consequences for
277 ingestion rate estimations are highly specific to the three study species and their ontogenetic
278 stage.

279 Our model predicts ingestion rates for *Z. scopas*, *B. undulatus* and *E. merra* at 15 cm TL to be
280 28.2 (11.7 – 68.4), 12.9 (3.7 – 56.7), 14.1 (5.5 – 40.1), respectively (in mg dry weight per g
281 wet weight of fish per day, median and 95% confidence interval (C.I.)) (see Appendix S2, Ta-
282 ble 2). Comparing our predicted excretion rates with empirical data on excretion rates shows
283 that our model adequately predicts excretion rates with almost all experimental data falling
284 inside the predicted 95% confidence interval (Fig. 4). For N excretion, 100%, 97% and 94%
285 of the experimental excretion rates are captured by our predictions for *Z. scopas*, *B. undulatus*
286 and *E. merra*, respectively. For P excretion, we adequately predict 93%, 94%, and 90% of the
287 experimental excretion rates for the three species, respectively. Predictions for *E. merra* are

288 slightly overestimated compared to experimental excretion rates. Groupers feed infrequently,
289 and their stomachs were often found empty, which may have impacted the measured excretion
290 rates.

291 Predictions are substantially affected by variability in the stoichiometry of dietary sources. To
292 illustrate how the diet stoichiometry affects limitations by different elements and ingestion
293 and excretion rates, we simulated different scenarios by varying the diet percentages of N and
294 P around the stoichiometry of the minimal supply rate of an individual of *Z. scopas* of 10 cm
295 (Fig. 5). When diet stoichiometry differs from this ideal stoichiometry of the minimal supply
296 rate, either C, N or P is the limiting element, which in turn affects all downstream biological
297 processes. For example, when the percent of P in the diet is low, P is the limiting element
298 (Fig. 5, A). This leads to an increased ingestion rate (Fig. 5, B), a minimal excretion rate of P
299 (Fig. 5, C), and a high excretion rate of N (Fig. 5, D).

300 Discussion

301 Combining stoichiometry and bioenergetic modeling provides a framework to predict elemen-
302 tal fluxes in consumers and their contribution to key biogeochemical cycles. Here, we intro-
303 duce a model that incorporates the nutrient requirements of fishes alongside their energetic
304 needs to provide accurate predictions of their ingestion, respiration, excretion, and egestion
305 rates. With our framework, we confirm the existence of nutrient limitation in fishes, specific
306 to the trophic group and life stage, and its effect on multiple processes. We demonstrate the
307 accuracy and applicability of the model to predict ingestion and excretion rates for three tropi-
308 cal reef fish species, while also reflecting the natural variability of these variables. Our frame-
309 work provides an accurate tool to predict CNP fluxes in fishes across diverse trophic groups
310 and gauge the role of fish consumers in ecosystems worldwide.

311 There is a growing consensus that many fishes are limited by nutrients (Benstead et al., 2014;
312 El-Sabaawi et al., 2016; Hood et al., 2005; Moody et al., 2019). Yet, fish growth and mainte-
313 nance are often assumed to be limited by energy (C) when applying coupled bioenergetic and
314 stoichiometric models (Allgeier et al., 2013; Burkepille et al., 2013; Kraft, 1992; Schindler &
315 Eby, 1997). Our case study confirms that ingestion rates can indeed be determined by N or P

316 limitation rather than C limitation, especially in species with nutrient-poor diets. This find-
317 ing is expected given the elemental imbalance between the consumer's body and dietary CNP
318 content; however, failing to account for nutrient limitation substantially skews predictions
319 of ingestion rates. For example, assuming only energy limitation for a herbivorous adult *Z.*
320 *scopas* would result in a greater than two-fold underestimation of its ingestion rate and con-
321 sequently drastic underestimations of excretion and egestion rates. Given the high densities
322 of species with nutrient-poor diets across a variety of ecosystems (e.g., herbivorous and de-
323 tritivorous species; Williams & Hatcher (1983); Takeuchi, Ochi, Kohda, Sinyinza, & Hori
324 (2010); Hood et al. (2005)), such underestimates may result in strong misconceptions about
325 ecosystem-scale nutrient and energy fluxes. Our model framework provides means for the
326 direct incorporation of varying elemental limitation across species.

327 The developed model predicts ingestion through the integration of metabolic theory and ele-
328 mental limitation, thus circumventing the difficult task of measuring ingestion rates in natural
329 populations. Therefore, the first step of our framework focuses on quantifying the minimal
330 supply rate for each element (S_k) and determining the limiting element. This includes both
331 maintenance rates and element-specific growth rates based on the growth trajectory of natu-
332 ral populations. Then, by comparing the stoichiometry of these minimal supply rates with diet
333 stoichiometry, we can determine the limiting element. This approach is inspired by thresh-
334 old elemental ratio (TER) theory, which predicts the ratio at which growth limitation switches
335 from one element to another (Sterner & Elser, 2002; Urabe & Watanabe, 1992). In fishes, it
336 is widely accepted to integrate metabolic rate into the calculation of TERs (Frost et al., 2006).
337 We built on this work to account not only for maintenance requirements of C, but also of N
338 and P. Similar to the energy (C) that is needed to sustain the metabolic rate of fishes in the
339 wild, minimal N and P is needed for cell turnover and maintenance of body composition.
340 The specific turnover rate of P (F_{0Pz}) is lower than the turnover rate of N (F_{0Nz}) because bone
341 cells, which contain the majority of P, degrade slowly compared to other cell types (Manola-
342 gas, 2000; Sterner & Elser, 2002). Thus, including minimal requirements for all three ele-
343 ments lowers the TER of C and nutrients of fishes and increases the probability of detecting
344 nutrient limitation.

345 The inclusion of nutrient limitation ensures that predicted excretion rates (F_P , F_N) are always
346 higher than zero. This is crucial since N and P will always be released at a minimal rate, even
347 when they are limiting (Anderson et al., 2005; Mayor et al., 2011; Sterner & Elser, 2002). Our
348 approach reveals that all three study species are limited by P in their early life. By explicitly
349 including minimal supply rates in our model, we move beyond simply detecting evidence for
350 nutrient limitation (i.e., negative excretion rates; Hood et al, 2005) towards quantifying its ef-
351 fect on vital processes across species and ontogeny. Bone growth, for example, requires sub-
352 stantial amounts of P and is most rapid during early life-stages (Vanni, 2002), and evidence
353 from freshwater ecosystems shows that P can limit fish growth (Benstead et al., 2014; Hood
354 et al., 2005). The ontogenetic variation in elemental limitation presented herein confirms the
355 importance of considering P-limitation for growth when predicting elemental fluxes in fishes.
356 Beyond the incorporation of nutrient limitation, our model framework provides a way to esti-
357 mate uncertainty of predictions. Empirically-measured excretion rates can considerably vary
358 for similarly sized individuals of the same species (Allgeier, Wenger, Rosemond, Schindler,
359 & Layman, 2015; Francis & Côté, 2018; Whiles, Huryn, Taylor, & Reeve, 2011). Yet, exist-
360 ing models that combine stoichiometry and bioenergetics do not account for this natural vari-
361 ability (e.g., Deslauriers et al., 2017), which hampers our ability to gauge the uncertainty of
362 resulting estimates. With the use of MCMC iterations, the R package `fishflux` incorporates
363 the distribution of parameters with their means and standard deviations, resulting in realistic
364 credibility intervals of ingestion and excretion rates, although variability in model output does
365 not necessarily reflect natural variability. The utility of this approach is clear when compar-
366 ing our predictions to reported ingestion rates. For example, *Z. scopas* reportedly ingests 49
367 mg of dry mass per gram of wet fish weight (Polunin, Harmelin-Vivien, & Galzin, 1995), a
368 value centered within the predicted range of our model (11.7 – 68.4 at 15 cm TL). Similarly,
369 the ingestion rate of juvenile coral trout, *Plectropomus leopardus*, a predatory species in the
370 same family as *E. merra* (family Serranidae), ranges between 9 to 14 mg of dry mass per gram
371 of wet weight (Sun et al., 2014), which lies within the 95% prediction for *E. merra* from our
372 model (5.5 – 40.1). Tracing the sensitivity of predictions to uncertainty in specific parameters
373 enables the determination of the main sources of variability that may shift estimates among

374 studies or species.

375 As all models, our approach relies on several simplifying assumptions. First, our model
376 assumes that fishes maintain homeostasis (Sterner, 1990). Since fishes can have flexible body
377 stoichiometry depending on dietary nutrient content (Benstead et al., 2014; Dalton et al.,
378 2017), this assumption may impose biases when simulating effects of varying diet stoichiometry
379 on elemental fluxes. Yet, empirically measured relationships between nutrient content
380 of body and diet can easily be incorporated into our model simulations, thus ameliorating the
381 effects of this simplification. Second, similar to most stoichiometric mass balance models,
382 our framework is based on Liebig's minimal rule, which states that growth is strictly limited
383 by the element in shortest supply relative to demand. However, there is emerging evidence
384 that consumers may simultaneously be limited by more than one element (Sperfeld, Martin-
385 Creuzburg, & Wacker, 2012). For example, P plays an essential role in fish energy uptake
386 (Xie et al., 2011), and the incorporation of interactive co-limitation into stoichiometric models
387 may further improve predictions of elemental fluxes. Finally, we assume that fishes follow a
388 growth trajectory defined by the VBGC curve, and that there is enough food available in the
389 natural environment to meet the growth requirements for each element. The VBGC is fitted
390 on size-at-age data that are mostly acquired via annual otolith readings. In our model, we use
391 this fitted growth function to estimate daily growth rates for each element through integration
392 with length-weight relationships and body stoichiometry. This does not capture, for instance,
393 seasonal variation of food availability. Other stoichiometric models mostly use gross growth
394 efficiencies (GGEs, i.e., growth/ingestion of the limiting element) (e.g., El-Sabaawi et al.,
395 2016; Frost et al., 2006; Guariento et al., 2018; McManamay, Webster, Valett, & Dolloff,
396 2011; Moody et al., 2019). However, consumer GGEs vary widely, and specific values are
397 poorly understood (McManamay et al., 2011). Furthermore, even if element-specific GGEs
398 are quantified, they may not reflect growth observed in natural populations. Therefore, we
399 suggest that the use of otolith-based growth quantification provides a reasonable alternative to
400 model elemental fluxes of natural fish populations.

401 Beyond model assumptions, the accuracy of our model naturally relies on the accuracy of each
402 parameter estimate. Yet, parameters are often difficult to obtain. We sought to balance the ac-

403 curacy of predictions and ease of application. Parameters involving growth, length-weight
404 relationships, metabolism, and stoichiometry are increasingly accessible for many species
405 due to predictive modeling and open-access databases (e.g., Froese, Thorson, & Reyes, 2014;
406 Barneche et al., 2014; Froese & Pauly, 2018; Killen et al., 2016; Morais & Bellwood, 2018;
407 Vanni et al., 2017). Yet, there are a number of parameters that are still sparsely quantified
408 and may limit the applicability of our framework. In particular, data on diet stoichiometry
409 and assimilation efficiencies are rare. In our case study, we used assimilation efficiency con-
410 stants for C, N and P, that are predominantly based on predatory fishes. In reality, assimi-
411 lation efficiencies can vary substantially, and, in particular, assimilation efficiency of phospho-
412 rus is likely correlated with diet quality (Czamanski et al., 2011). Further, N- and P-specific
413 turnover rates are newly introduced parameters and therefore poorly known. As these param-
414 eters depend on the cell turnover rates of N- and P-rich tissues (e.g., bone cells for P), we sug-
415 gest that these parameters may be applicable across species. Nevertheless, further research is
416 needed to gain more insight. While variation in these parameters can impact the model out-
417 put via the limiting element and ingestion rate, ongoing compilations of databases of poorly
418 known parameters will improve the application of the proposed modeling framework.

419 In addition, we quantified the activity scope (i.e., field metabolic rate) as the average of
420 maximum metabolic rates (MMR) and standard metabolic rates (SMR) divided by the SMR,
421 assuming that a fish reaches values close to MMR when undertaking activities in the wild
422 (Murchie, Cooke, Danylchuk, & Suski, 2011). In reality, activity scope may vary depending
423 on life history traits and behavior (Killen, Norin, & Halsey, 2017), and field metabolic rates
424 can be elevated with the presence of predators, which in turn can affect nutrient cycling
425 (Dalton, Tracy, Hairston, & Flecker, 2018; Guariento et al., 2018). Refining established
426 techniques, such as bio-telemetry (Norin & Clark, 2016) or otolith chemistry (Chung,
427 Trueman, Godiksen, Holmstrup, & GrønkJær, 2019) may improve estimates of field metabolic
428 rates. Similarly, specific dynamic action (SDA), which is the metabolic rate needed to
429 assimilate food (Hou et al., 2008) depends on the quality and quantity of food (McCue, 2006)
430 and may thus influence ingestion rates, but it is poorly known across most species. Finally,
431 reproduction is not yet incorporated into the model because data on both gonad stoichiometry

432 and reproductive growth is rare. This may underestimate energy and nutrient investment of
433 fishes, thus skewing model predictions. Nonetheless, as new data on reproductive growth,
434 activity scope, or SDA become available, these elements can be incorporated in the future.

435 Despite these limitations, our framework provides new avenues for addressing pressing ques-
436 tions in ecology. Data on the daily actions of fishes are difficult to obtain due to the chal-
437 lenges of conducting research in aquatic environments. Novel techniques such as fish gut
438 content DNA metabarcoding (Casey et al., 2019) or compound-specific stable isotope anal-
439 yses (Hopkins & Ferguson, 2012) permit improved insights into species-specific ingestion
440 of prey resources. However, no current empirical technique can estimate rates of food inges-
441 tion via these linkages across a broad range of species. Combining our model with emerging
442 techniques to quantify species-specific resource use can help us to address long standing ques-
443 tions. How much prey do top predators consume daily? How do rates of algal consumption
444 differ among herbivorous species? How much production by lower trophic levels is needed to
445 fuel the growth of predatory fisheries species? By providing a tool to answer these questions,
446 our model empowers fundamental and applied researchers to tackle some of the most impor-
447 tant questions in fish ecology.

448 Beyond single species and their pairwise interactions, our model provides means to examine
449 community- and ecosystem-scale dynamics. Specifically, based on simple census data of fish
450 communities, our model can help decompose system-wide fluxes (cf. Burkepille et al., 2013;
451 Allgeier et al., 2014; Francis & Côté, 2018). This is particularly important for open ecosys-
452 tems in which the dominant sources of energy and nutrients are unclear or variable. For exam-
453 ple, on coral reefs, debates persist on the importance of external (i.e., pelagic) subsidies versus
454 internal nutrient cycling (e.g., Brandl, Tornabene, et al., 2019; Morais & Bellwood, 2019).

455 Our model can help estimate how much pelagic or benthic prey is consumed by reef fishes and
456 how these resources are propagated through food webs, which enables researchers to quantify
457 reef functioning (Brandl, Rasher, et al., 2019). Thus, merging what is eaten (i.e., food web as-
458 sembly) with how much is eaten (i.e., realistic consumption rates as provided by our model)
459 can significantly augment our understanding of ecosystem functioning, especially in systems
460 where fishes are the dominant consumers.

461 Finally, given the heavy exploitation of fish communities for global human consumption, our
462 model offers a tool for understanding and predicting the effect of human-driven changes on
463 ecosystem functioning. Yearly, more than 100 million tons of fishes are caught in marine sys-
464 tems worldwide (Cashion et al., 2018). Our model provides a tool to estimate the impact of
465 this disturbance on system-wide biogeochemical fluxes. In addition, increasing tempera-
466 tures resulting from climate change can affect primary production in the world's oceans, thus
467 imposing a bottom-up effect on fish communities (Lotze et al., 2019), which are likewise af-
468 fected by rising temperatures (Pinsky, Eikeset, McCauley, Payne, & Sunday, 2019). Given
469 human-driven alterations in both primary production through climate change and fish com-
470 munity structure through extensive fishing, it is urgent to understand how these changes may
471 impact biogeochemical fluxes. Our model and its implementation provide a path toward rising
472 to this challenge.

473 **Data accessibility**

474 All data and code to reproduce figures are available online at

475 <https://zenodo.org/record/3894509#.XuysMZZS-V4>.

476 The R package `fishflux`, containing the model can be installed through GitHub:

477 <https://github.com/nschielt/fishflux>.

478 **Supporting information**

479 Appendix S1 (Supplementary methods)

480 Appendix S2 (Supplementary tables)

481 **Figure legends**

482 **Figure 1.** Conceptual diagram, explaining different model components. Required ingestion
483 of C, N and P is calculated through the sum of elements needed for growth and minimal in-
484 organic flux, taking into account the element-specific assimilation efficiencies, a_k (1). Based
485 on the limiting element (due to the imbalance of food and the required CNP), the ingestion
486 rate can be estimated (2). The ingested material is partitioned into egestion (3) and assimi-
487 lation (body mass growth and flux (4)). The symbol of each component is indicated in between
488 brackets. The input parameters needed to calculate the different variables are italicised. See
489 Table 1 for a description of each parameter.

490 **Figure 2.** Proportion of the simulation iterations that determine C, N and P as the limiting
491 element for *Zebrasoma scopas*, *Balistapus undulatus*, and *Epinephelus merra*.

492 **Figure 3.** Predicted daily ingestion of carbon and excretion rates for the full model, consider-
493 ing nutrient limitation and for a model, only taking into account C-limitation. Horizontal lines
494 show the median values and 95%, 80%, and 50% confidence intervals are illustrated respec-
495 tively in vertical lines. A. C ingestion rates of *Z. scopas*, B. N excretion rates of *Z. scopas*, C.
496 P excretion rates of *Z. scopas*, D. C ingestion rates of *B. undulatus*, E. N excretion rates of *B.*
497 *undulatus*, F. P excretion rates of *B. undulatus*, G. C ingestion rates of *E. merra*, H. N excre-
498 tion rates of *E. merra*, I. P excretion rates of *E. merra*.

499 **Figure 4.** Predicted excretion rates for each species of both N and P. The 50%, 80% and 95%
500 confidence intervals are presented around the median. Points show the experimental excretion
501 rates, obtained from an independent database. A. N excretion rates of *Z. scopas*, B. P excre-
502 tion rates of *Z. scopas*, C. N excretion rates of *B. undulatus*, D. P excretion rates of *B. undula-*
503 *tus*, E. N excretion rates of *E. merra*, F. P excretion rates of *E. merra*.

504 **Figure 5.** Model simulations with varying levels of D_N and D_P . D_C is kept constant. Diet
505 stoichiometry affects the limitation and the rates of multiple processes, such as the ingestion
506 rate and excretion rates. A. The limiting element is indicated for varying levels of diet stoi-
507 chiometry (D_N and D_P). Lines indicate where one limiting element switches to another. This
508 is equivalent to the threshold elemental ratio, B. I_C or Ingestion rates of C (g/day), C. F_N or

509 Total inorganic flux of N (g/day), D. F_p or Total inorganic flux of P (g/day).

Author Manuscript

510 **References**

- 511 Allgeier, J. E., Layman, C. A., Mumby, P. J., & Rosemond, A. D. (2014). Consistent nutrient
512 storage and supply mediated by diverse fish communities in coral reef ecosystems. *Global*
513 *Change Biology*, *20*(8), 2459–2472. doi: 10.1111/gcb.12566
- 514 Allgeier, J. E., Wenger, S. J., Rosemond, A. D., Schindler, D. E., & Layman, C. A. (2015).
515 Metabolic theory and taxonomic identity predict nutrient recycling in a diverse food
516 web. *Proceedings of the National Academy of Sciences*, *112*(20), E2640–E2647. doi:
517 10.1073/pnas.1420819112
- 518 Allgeier, J. E., Yeager, L. A., & Layman, C. A. (2013). Consumers regulate nutrient limita-
519 tion regimes and primary production in seagrass ecosystems. *Ecology*, *94*(2), 521–529. doi:
520 10.1890/12-1122.1
- 521 Anderson, T. R., Hessen, D. O., Elser, J. J., & Urabe, J. (2005). Metabolic stoichiometry and
522 the fate of excess Carbon and Nutrients in Consumers. *The American Naturalist*, *165*(1), 1–
523 15. doi: 10.1086/426598
- 524 Barneche, D. R., & Allen, A. P. (2018). The energetics of fish growth and how it constrains
525 food-web trophic structure. *Ecology Letters*, *21*(6), 836–844. doi: 10.1111/ele.12947
- 526 Barneche, D. R., Kulbicki, M., Floeter, S. R., Friedlander, A. M., Maina, J., & Allen, A. P.
527 (2014). Scaling metabolism from individuals to reef-fish communities at broad spatial scales.
528 *Ecology Letters*, *17*(9), 1067–1076. doi: 10.1111/ele.12309
- 529 Benstead, J. P., Hood, J. M., Whelan, N. V., Kendrick, M. R., Nelson, D., Hanninen, A. F.,
530 & Demi, L. M. (2014). Coupling of dietary phosphorus and growth across diverse fish taxa:
531 A meta-analysis of experimental aquaculture studies. *Ecology*, *95*(10), 2768–2777. doi:
532 10.1890/13-1859.1
- 533 Bertalanffy, L. von. (1957). Quantitative laws in metabolism and growth. *The Quarterly Re-*
534 *view of Biology*, *32*, 217–231. doi: 10.1086/401873
- 535 Brandl, Rasher, D. B., Côté, I. M., Casey, J. M., Darling, E. S., Lefcheck, J. S., & Duffy, J. E.
536 (2019). Coral reef ecosystem functioning: Eight core processes and the role of biodiversity.

537 *Frontiers in Ecology and the Environment*, 17(8), 445–454. doi: 10.1002/fee.2088

538 Brandl, Tornabene, L., Goatley, C. H. R., Casey, J. M., Morais, R. A., Côté, I. M., ... Bell-
539 wood, D. R. (2019). Demographic dynamics of the smallest marine vertebrates fuel coral reef
540 ecosystem functioning. *Science*, 364(6446), 1189–1192. doi: 10.1126/science.aav3384

541 Brown, J. H., Gillooly, J. F., Allen, A. P., Savage, V. M., & West, G. B. (2004). Toward a
542 metabolic theory of ecology. *Ecology*, 85(7), 1771–1789. doi: Doi 10.1890/03-9000

543 Burkepile, D. E., Allgeier, J. E., Shantz, A. A., Pritchard, C. E., Lemoine, N. P., Bhatti,
544 L. H., & Layman, C. A. (2013). Nutrient supply from fishes facilitates macroalgae and
545 suppresses corals in a Caribbean coral reef ecosystem. *Scientific Reports*, 3(1), 1493. doi:
546 10.1038/srep01493

547 Capps, K. A., & Flecker, A. S. (2013). Invasive Fishes Generate Biogeochemical Hotspots in
548 a Nutrient-Limited System. *PLoS ONE*, 8(1), e54093. doi: 10.1371/journal.pone.0054093

549 Casey, J. M., Meyer, C. P., Morat, F., Brandl, S. J., Planes, S., & Parravicini, V. (2019).
550 Reconstructing hyperdiverse food webs: gut content metabarcoding as a tool to disentangle
551 trophic interactions on coral reefs. *Methods in Ecology and Evolution*, 00, 1–14. doi:
552 10.1111/2041-210X.13206

553 Cashion, T., Al-Abdulrazzak, D., Belhabib, D., Derrick, B., Divovich, E., Moutopoulos,
554 D. K., ... Pauly, D. (2018). Reconstructing global marine fishing gear use: Catches
555 and landed values by gear type and sector. *Fisheries Research*, 206, 57–64. doi:
556 10.1016/j.fishres.2018.04.010

557 Chung, M.-T., Trueman, C. N., Godiksen, J. A., Holmstrup, M. E., & Grønkjær, P. (2019).
558 Field metabolic rates of teleost fishes are recorded in otolith carbonate. *Communications Biol-*
559 *ogy*, 2(1), 24. doi: 10.1038/s42003-018-0266-5

560 Czamanski, M., Nugraha, A., Pondaven, P., Lasbleiz, M., Masson, A., Caroff, N., ... Tréguer,
561 P. (2011). Carbon, nitrogen and phosphorus elemental stoichiometry in aquacultured and wild-
562 caught fish and consequences for pelagic nutrient dynamics. *Marine Biology*, 158(12), 2847–
563 2862. doi: 10.1007/s00227-011-1783-7

564 Dalton, C. M., El-Sabaawi, R. W., Honeyfield, D. C., Auer, S. K., Reznick, D. N., & Flecker,
565 A. S. (2017). The influence of dietary and whole-body nutrient content on the excretion of a
566 vertebrate consumer. *PLoS ONE*, *12*(1), e0187931. doi: 10.1371/journal.pone.0187931

567 Dalton, C. M., Tracy, K. E., Hairston, N. G., & Flecker, A. S. (2018). Fasting or fear: disen-
568 tangling the roles of predation risk and food deprivation in the nitrogen metabolism of con-
569 sumers. *Ecology*, *99*(3), 681–689. doi: 10.1002/ecy.2132

570 Deslauriers, D., Chipps, S. R., Breck, J. E., Rice, J. A., & Madenjian, C. P. (2017). Fish
571 Bioenergetics 4.0: An R-Based Modeling Application. *Fisheries*, *42*(11), 586–596. doi:
572 10.1080/03632415.2017.1377558

573 Elliott, J. M., & Persson, L. (1978). The Estimation of Daily Rates of Food Consumption for
574 Fish. *The Journal of Animal Ecology*, *47*(3), 977–991. doi: 10.2307/3682

575 El-Sabaawi, R. W., Warbanski, M. L., Rudman, S. M., Hovel, R., & Matthews, B. (2016).
576 Investment in boney defensive traits alters organismal stoichiometry and excretion in fish. *Oe-*
577 *cologia*, *181*(4), 1209–1220. doi: 10.1007/s00442-016-3599-0

578 Francis, F. T., & Côté, I. M. (2018). Fish movement drives spatial and temporal patterns of
579 nutrient provisioning on coral reef patches. *Ecosphere*, *9*(5), e02225. doi: 10.1002/ecs2.2225

580 Froese, R., & Pauly, D. (2018). FishBase. *World Wide Web Electronic Publication*.

581 Froese, R., Thorson, J. T., & Reyes, R. B. (2014). A Bayesian approach for estimating
582 length-weight relationships in fishes. *Journal of Applied Ichthyology*, *30*(1), 78–85. doi:
583 10.1111/jai.12299

584 Frost, P. C., Benstead, J. P., Cross, W. F., Hillebrand, H., Larson, J. H., Xenopoulos, M. A.,
585 & Yoshida, T. (2006). Threshold elemental ratios of carbon and phosphorus in aquatic con-
586 sumers. *Ecology Letters*, *9*(7), 774–779. doi: 10.1111/j.1461-0248.2006.00919.x

587 Graham, N. A., McClanahan, T. R., MacNeil, M. A., Wilson, S. K., Cinner, J. E., Huchery, C.,
588 & Holmes, T. H. (2017). Human Disruption of Coral Reef Trophic Structure. *Current Biology*,
589 *27*(2), 231–236. doi: 10.1016/j.cub.2016.10.062

590 Guariento, R. D., Luttbeg, B., Carneiro, L. S., & Caliman, A. (2018). Prey adaptive behaviour

591 under predation risk modify stoichiometry predictions of predator-induced stress paradigms.
592 *Functional Ecology*, 32(6), 1631–1643. doi: 10.1111/1365-2435.13089

593 Hanson, P., Johnson, T. B., Schindler, D. E., & Kitchell, J. F. (1997). *Fish Bioenergetics 3.0*.

594 Hessen, D. O., Ågren, G. I., Anderson, T. R., Elser, J. J., & De Ruiter, P. C. (2004). Carbon
595 sequestration in ecosystems: The role of stoichiometry. *Ecology*, 85(5), 1179–1192. doi:
596 10.1890/02-0251

597 Hood, J. M., Vanni, M. J., & Flecker, A. S. (2005). Nutrient recycling by two phosphorus-rich
598 grazing catfish: The potential for phosphorus-limitation of fish growth. *Oecologia*, 146(2),
599 247–257. doi: 10.1007/s00442-005-0202-5

600 Hopkins, J. B., & Ferguson, J. M. (2012). Estimating the Diets of Animals Using Stable
601 Isotopes and a Comprehensive Bayesian Mixing Model. *PLoS ONE*, 7(1), e28478. doi:
602 10.1371/journal.pone.0028478

603 Hou, C., Zuo, W., Moses, M. E., Woodruff, W. H., Brown, J. H., & West, G. B. (2008).
604 Energy Uptake and Allocation During Ontogeny. *Science*, 322(5902), 736–739. doi:
605 10.1126/science.1162302

606 Killen, S. S., Glazier, D. S., Rezende, E. L., Clark, T. D., Atkinson, D., Willener, A. S. T.,
607 & Halsey, L. G. (2016). Ecological Influences and Morphological Correlates of Resting and
608 Maximal Metabolic Rates across Teleost Fish Species. *The American Naturalist*, 187(5), 592–
609 606. doi: 10.1086/685893

610 Killen, S. S., Norin, T., & Halsey, L. G. (2017). Do method and species lifestyle affect mea-
611 sures of maximum metabolic rate in fishes? *Journal of Fish Biology*, 90(3), 1037–1046. doi:
612 10.1111/jfb.13195

613 Kitchell, J. F., Koonce, J. F., Magnuson, J. J., O'Neill, R. V., Shugart, H. H., & Booth, R. S.
614 (1974). Model of fish biomass dynamics. *Transactions of the American Fisheries Society*,
615 103(4), 786–798. doi: 10.1577/1548-8659(1974)103<786:MOFBD>2.0.CO;2

616 Kooijman, S. (2010). Dynamic energy budget theory - summary of concepts of the
617 third edition. *Dynamic Energy Budget Theory for Metabolilc Organization*, 64. doi:

618 10.1017/CBO9780511565403

619 Kraft, C. (1992). Estimates of phosphorus and nitrogen cycling by fish using a bioenerget-
620 ics approach. *Canadian Journal of Fisheries and Aquatic Sciences*, 49(12), 2596–2604. doi:
621 10.1139/f92-287

622 Lotze, H. K., Tittensor, D. P., Bryndum-Buchholz, A., Eddy, T. D., Cheung, W. W. L., Gal-
623 braith, E. D., ... Worm, B. (2019). Global ensemble projections reveal trophic amplification
624 of ocean biomass declines with climate change. *Proceedings of the National Academy of Sci-
625 ences*, 116(26), 12907–12912. doi: 10.1073/PNAS.1900194116

626 Mackenzie, F. T., Ver, L. M., Sabine, C., Lane, M., & Lerman, A. (1993). C, N, P, S Global
627 Biogeochemical Cycles and Modeling of Global Change. In *Interactions of c, n, p and s bio-
628 geochemical cycles and global change* (pp. 1–61). doi: 10.1007/978-3-642-76064-8_1

629 Manolagas, S. C. (2000). Birth and Death of Bone Cells: Basic Regulatory Mechanisms and
630 Implications for the Pathogenesis and Treatment of Osteoporosis 1. *Endocrine Reviews*, 21(2),
631 115–137. doi: 10.1210/edrv.21.2.0395

632 Mayor, D. J., Cook, K., Thornton, B., Walsham, P., Witte, U. F., Zuur, A. F., & Ander-
633 son, T. R. (2011). Absorption efficiencies and basal turnover of C, N and fatty acids in a
634 marine Calanoid copepod. *Functional Ecology*, 144(4), 381–394. doi: 10.1111/j.1365-
635 2435.2010.01791.x

636 McCue, M. D. (2006). Specific dynamic action: A century of investigation. *Comparative Bio-
637 chemistry and Physiology - A Molecular and Integrative Physiology*, 144(4), 381–394. doi:
638 10.1016/j.cbpa.2006.03.011

639 McIntyre, P. B., Flecker, A. S., Vanni, M. J., Hood, J. M., Taylor, B. W., & Thomas, S. A.
640 (2008). Fish distributions and nutrient cycling in streams: can fish create biogeochemical
641 hotspots. *Ecology*, 89(8), 2335–2346. doi: 10.1890/07-1552.1

642 McManamay, R. A., Webster, J. R., Valett, H. M., & Dolloff, C. A. (2011). Does diet influ-
643 ence consumer nutrient cycling? Macroinvertebrate and fish excretion in streams. *Journal of
644 the North American Benthological Society*, 30(1), 84–102. doi: 10.1899/09-152.1

- 645 Moody, E. K., Carson, E. W., Corman, J. R., Espinosa-Pérez, H., Ramos, J., Sabo, J. L., &
646 Elser, J. J. (2018). Consumption explains intraspecific variation in nutrient recycling stoi-
647 chiometry in a desert fish. *Ecology*, *99*(7), 1552–1561. doi: 10.1002/ecy.2372
- 648 Moody, E. K., Lujan, N. K., Roach, K. A., & Winemiller, K. O. (2019). Threshold elemental
649 ratios and the temperature dependence of herbivory in fishes. *Functional Ecology*, *33*(5), 913–
650 923. doi: 10.1111/1365-2435.13301
- 651 Morais, R. A., & Bellwood, D. R. (2018). Global drivers of reef fish growth. *Fish and Fish-*
652 *eries*, *19*(5), 874–889. doi: 10.1111/faf.12297
- 653 Morais, R. A., & Bellwood, D. R. (2019). Pelagic Subsidies Underpin Fish Pro-
654 ductivity on a Degraded Coral Reef. *Current Biology*, *29*(9), 1521–1527.e6. doi:
655 10.1016/J.CUB.2019.03.044
- 656 Murchie, K. J., Cooke, S. J., Danylchuk, A. J., & Suski, C. D. (2011). Estimates of field activ-
657 ity and metabolic rates of bonefish (*Albula vulpes*) in coastal marine habitats using acoustic
658 tri-axial accelerometer transmitters and intermittent-flow respirometry. *Journal of Experimen-*
659 *tal Marine Biology and Ecology*, *396*(2), 147–155. doi: 10.1016/j.jembe.2010.10.019
- 660 Norin, T., & Clark, T. D. (2016). Measurement and relevance of maximum metabolic rate in
661 fishes. *Journal of Fish Biology*, *88*(1), 122–151. doi: 10.1111/jfb.12796
- 662 Odum, H. T., & Odum, E. P. (1955). Trophic Structure and Productivity of a Windward
663 Coral Reef Community on Eniwetok Atoll. *Ecological Monographs*, *25*(3), 291–320. doi:
664 10.2307/1943285
- 665 Pinsky, M. L., Eikeset, A. M., McCauley, D. J., Payne, J. L., & Sunday, J. M. (2019). Greater
666 vulnerability to warming of marine versus terrestrial ectotherms. *Nature*, *569*(7754), 108–111.
667 doi: 10.1038/s41586-019-1132-4
- 668 Polunin, N. V., Harmelin-Vivien, M., & Galzin, R. (1995). Contrasts in algal food process-
669 ing among five herbivorous coral-reef fishes. *Journal of Fish Biology*, *47*(3), 455–465. doi:
670 10.1111/j.1095-8649.1995.tb01914.x
- 671 R Core Team. (2019). *R: A language and environment for statistical computing*. Retrieved

672 from <https://www.R-project.org/>

673 Schiettekatte, N., Brandl, S., & Casey, J. (2019). *Fishualize: Color palettes based on fish*
674 *species*. Retrieved from <https://github.com/nschiett/fishualize>

675 Schindler, D. E., & Eby, L. A. (1997). Stoichiometry of fishes and their prey: Im-
676 plications for nutrient recycling. *Ecology*, 78(6), 1816–1831. doi: 10.1890/0012-
677 9658(1997)078[1816:SOFATP]2.0.CO;2

678 Schreck, C. B., & Moyle, P. B. (1990). *Methods for Fish Biology* (pp. 1–387).

679 Sperfeld, E., Martin-Creuzburg, D., & Wacker, A. (2012). Multiple resource limitation the-
680 ory applied to herbivorous consumers: Liebig’s minimum rule vs. interactive co-limitation.
681 *Ecology Letters*, 15(2), 142–150. doi: 10.1111/j.1461-0248.2011.01719.x

682 Stan Development Team. (2018). *RStan: the R interface to Stan. R package version 2.17.3*.
683 doi: 10.3168/jds.S0022-0302(63)89186-9

684 Sterner, R., & Elser, J. (2002). *Ecological Stoichiometry: The Biology of Elements from*
685 *Molecules to the Biosphere* (pp. 1–439). Retrieved from [https://press.princeton.edu/](https://press.princeton.edu/titles/7434.html)
686 [titles/7434.html](https://press.princeton.edu/titles/7434.html)

687 Sterner, R. W. (1990). The ratio of nitrogen to phosphorus resupplied by herbivores:
688 zooplankton and the algal competitive arena. *American Naturalist*, 136(2), 209–229. doi:
689 10.1086/285092

690 Sun, Z., Xia, S., Feng, S., Zhang, Z., Rahman, M. M., Rajkumar, M., & Jiang, S. (2014). Ef-
691 fects of water temperature on survival, growth, digestive enzyme activities, and body com-
692 position of the leopard coral grouper *Plectropomus leopardus*. *Fisheries Science*, 81(1), 107–
693 112. doi: 10.1007/s12562-014-0832-9

694 Takeuchi, Y., Ochi, H., Kohda, M., Sinyinza, D., & Hori, M. (2010). A 20-year census of a
695 rocky littoral fish community in Lake Tanganyika. *Ecology of Freshwater Fish*, 19(2), 239–
696 248. doi: 10.1111/j.1600-0633.2010.00408.x

697 Urabe, J., & Watanabe, Y. (1992). Possibility of N or P limitation for planktonic clado-
698 cerans: An experimental test. *Limnology and Oceanography*, 37(2), 244–251. doi:

699 10.4319/lo.1992.37.2.0244

700 Vanni, M. J. (2002). Nutrient Cycling by Animals in Freshwater Ecosystems. *Annual Review*
701 *of Ecology and Systematics*, 33(1), 341–370. doi: 10.1146/annurev.ecolsys.33.010802.150519

702 Vanni, M. J., McIntyre, P. B., Allen, D., Arnott, D. L., Benstead, J. P., Berg, D. J., ... Zim-
703 mer, K. D. (2017). A global database of nitrogen and phosphorus excretion rates of aquatic
704 animals. *Ecology*, 98, 1475. doi: 10.1002/ecy.1792

705 Welti, N., Striebel, M., Ulseth, A. J., Cross, W. F., DeVilbiss, S., Glibert, P. M., ... Hille-
706 brand, H. (2017). Bridging food webs, ecosystem metabolism, and biogeochemistry
707 using ecological stoichiometry theory. *Frontiers in Microbiology*, 8(JUL), 1298. doi:
708 10.3389/fmicb.2017.01298

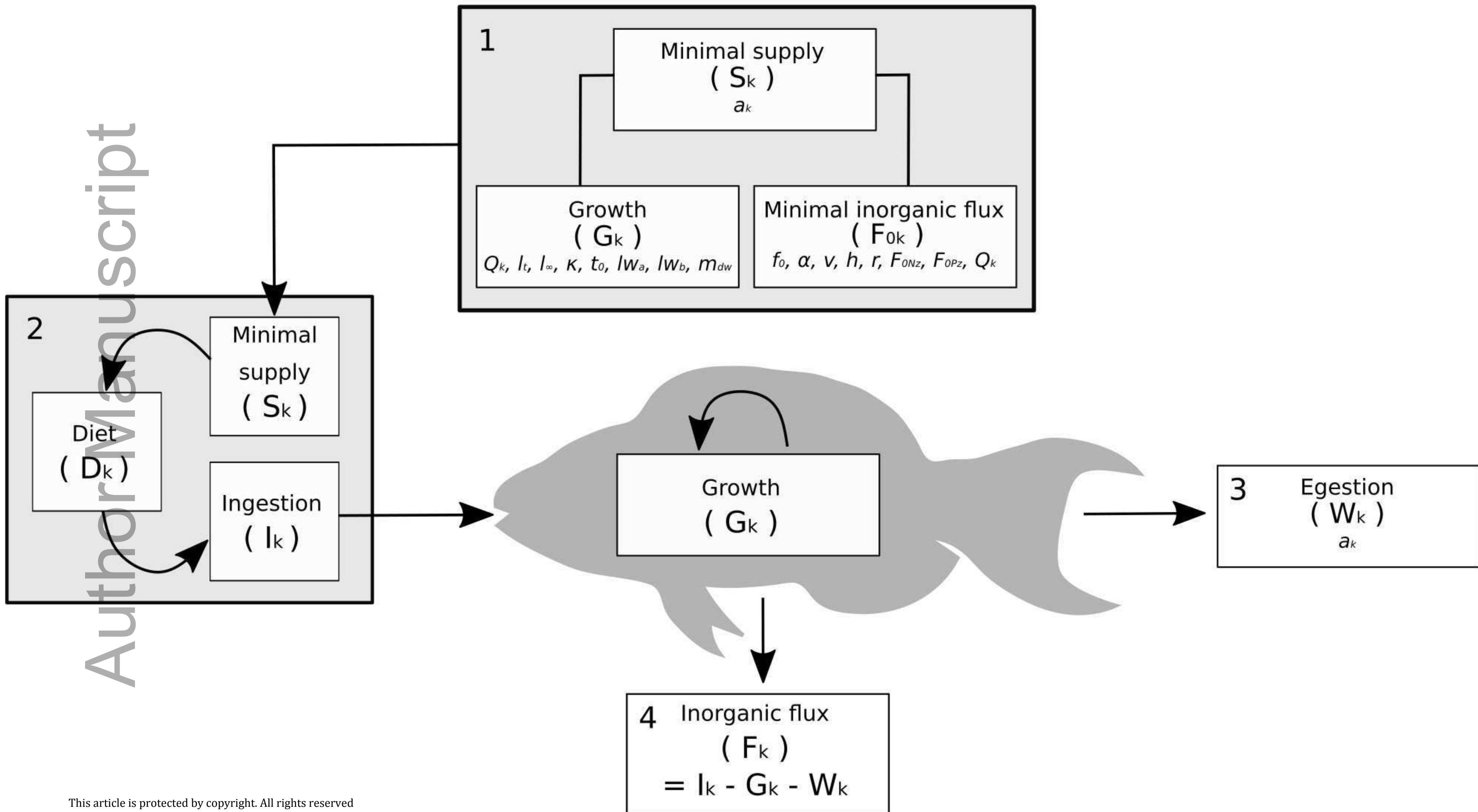
709 Whiles, M. R., Hury, A. D., Taylor, B. W., & Reeve, J. D. (2011). Influence of handling
710 stress and fasting on estimates of ammonium excretion by tadpoles and fish: recommenda-
711 tions for designing excretion experiments. *Limnology and Oceanography: Methods*, 7(1),
712 1–7. doi: 10.4319/lom.2009.7.1

713 Williams, D., & Hatcher, A. (1983). Structure of Fish Communities on Outer Slopes of In-
714 shore, Mid-Shelf and Outer Shelf Reefs of the Great Barrier Reef. *Marine Ecology Progress*
715 *Series*, 10, 239–250. doi: 10.3354/meps010239

716 Xie, N. B., Feng, L., Liu, Y., Jiang, J., Jiang, W. D., Hu, K., ... Zhou, X. Q. (2011). Growth,
717 body composition, intestinal enzyme activities and microflora of juvenile Jian carp (*Cyprinus*
718 *carpio* var. Jian) fed graded levels of dietary phosphorus. *Aquaculture Nutrition*, 17, 645–656.
719 doi: 10.1111/j.1365-2095.2011.00867.x

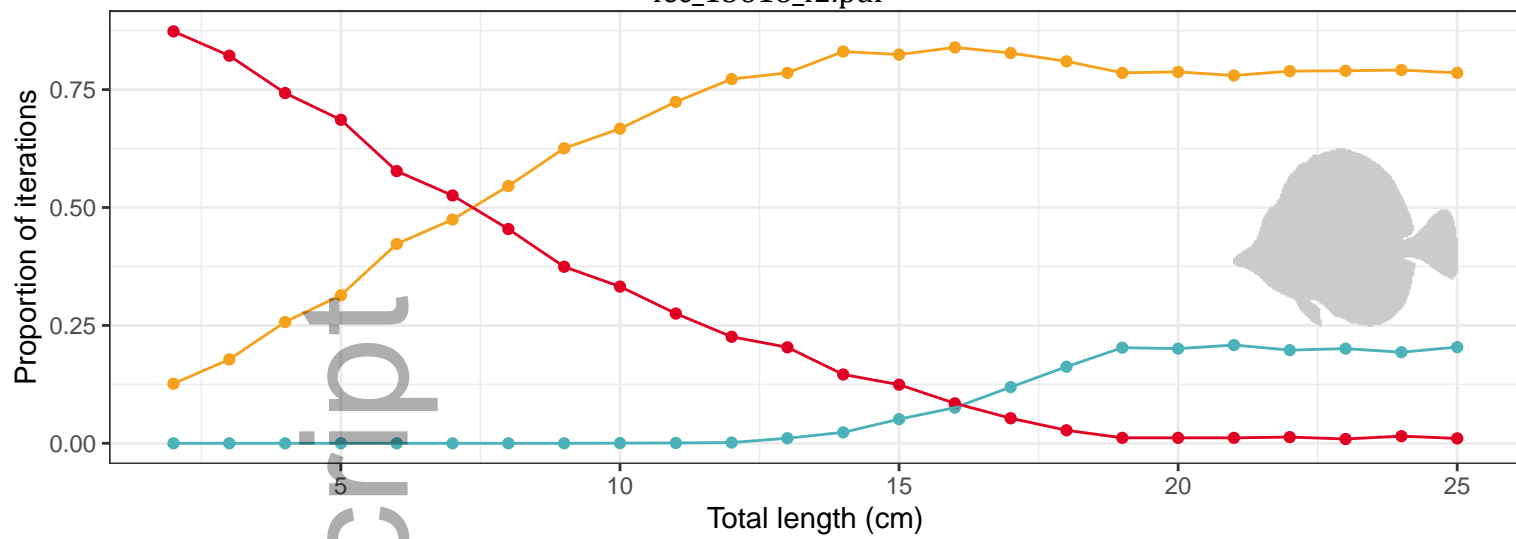
Table 1. Overview of model parameters and variables, including input parameters, to be specified by the user of the model, which are indicated with *. Main output variables, predicted by the model are indicated with ▲. VBGC = von Bertalanffy growth curve.

Symbol	Description	Unit
k	Index for element C, N or P	–
S_k ▲	Element-specific minimal supply rate	g d^{-1}
G_k ▲	Element-specific growth	g d^{-1}
F_{0k} ▲	Element-specific minimal inorganic flux	g d^{-1}
a_k *	Element-specific assimilation efficiency	–
l_t *	Total length of individual at time t	cm
t	Age	yr
l_∞ *	Asymptotic adult length (VBGC)	cm
κ *	Growth rate parameter (VBGC)	yr^{-1}
t_0 *	Age at settlement (VBGC)	yr
lw_a *	Parameter length-weight relationship	g cm^{-1}
lw_b *	Parameter length-weight relationship	–
Q_k *	Element-specific body content percentage of dry mass	%
m_w	Wet body mass	g
F_{0Cr}	Resting metabolic rate	g d^{-1}
F_{0Cz}	Mass-specific turnover rate of C	$\text{g C g}^{-1} \text{d}^{-1}$
F_{0Cs}	Rate of C spent in body mass growth	g d^{-1}
f_0 *	Metabolic normalisation constant independent of body mass	$\text{g C g}^{-\alpha} \text{d}^{-1}$
α *	Mass-scaling exponent	–
$m_{w\infty}$	Asymptotic wet mass of an adult individual	g
ϕ	Cost of growth	g C g^{-1}
θ *	Activity scope	–
v *	Environmental temperature	$^{\circ}\text{C}$
h *	trophic level	–
r *	Aspect ratio of caudal fin	–
F_{0Nz} *	Mass-specific turnover rate of N	$\text{g Ng}^{-1} \text{d}^{-1}$
F_{0Pz} *	Mass-specific turnover rate of P	$\text{g Pg}^{-1} \text{d}^{-1}$
m_{dw}	Ratio of dry mass and wet mass of fish	–
m_d	Dry body mass	g
D_k *	Element-specific diet content percentage of dry mass	%
I_k ▲	Element-specific ingestion rate	g d^{-1}
W_k ▲	Element-specific egestion rate	g d^{-1}
F_{rk} ▲	Element-specific residual inorganic flux	g d^{-1}
F_k ▲	Element-specific total inorganic flux	g d^{-1}

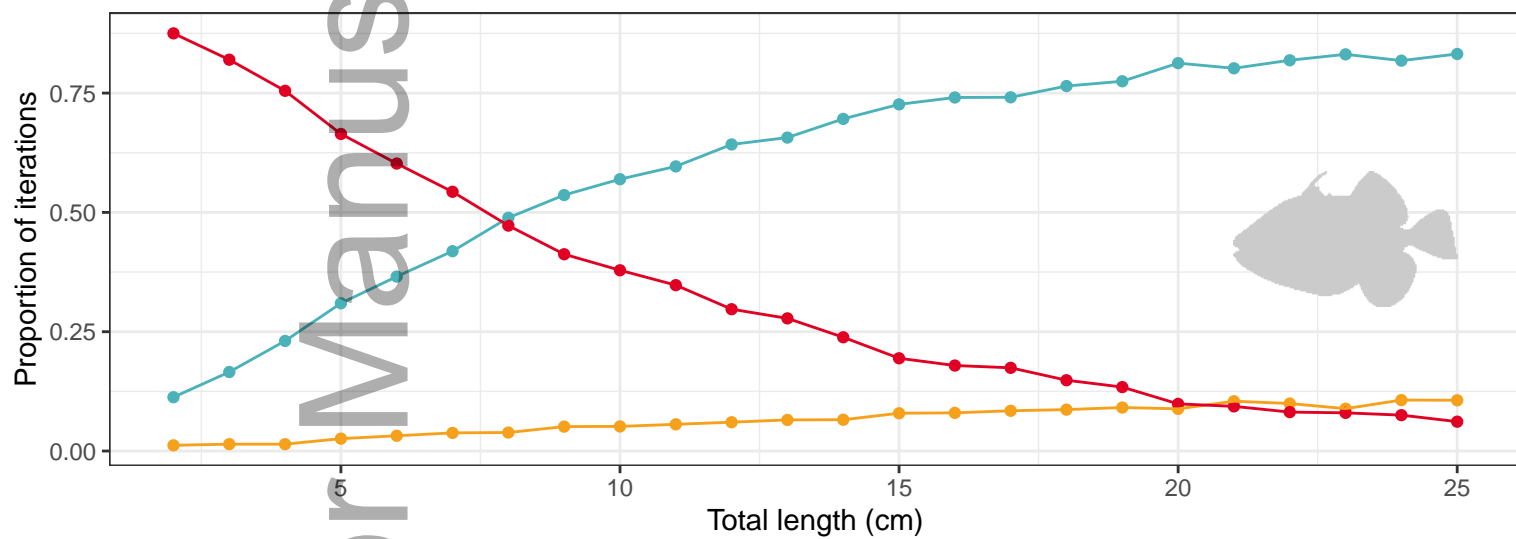


Z. scopas

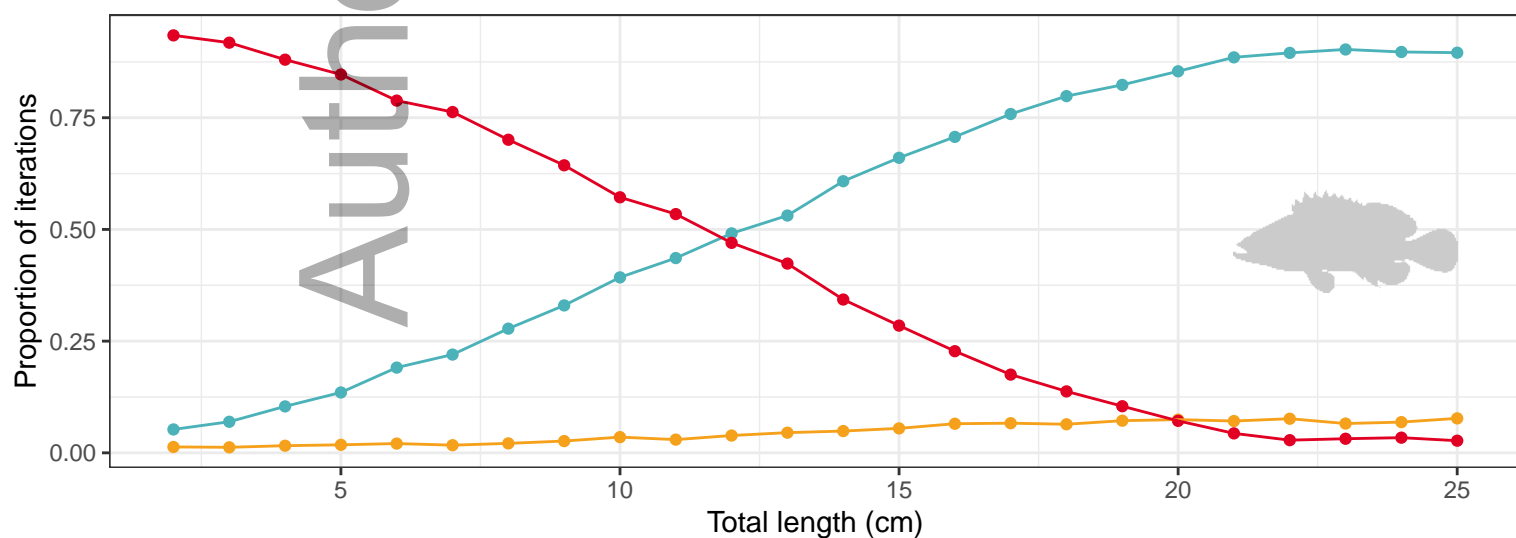
fec_13618_f2.pdf



B. undulatus

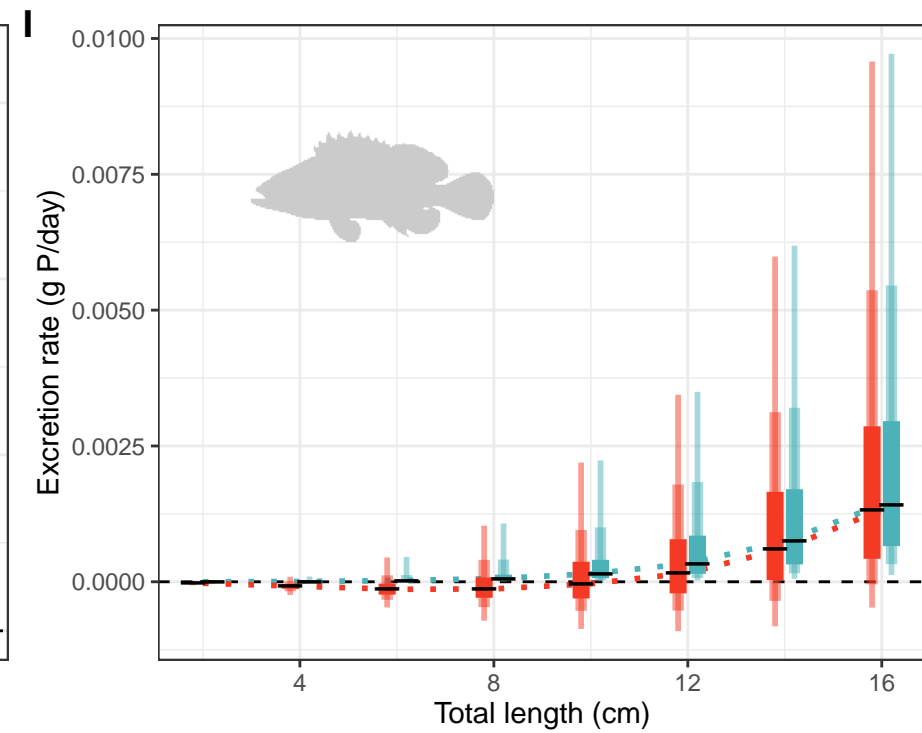
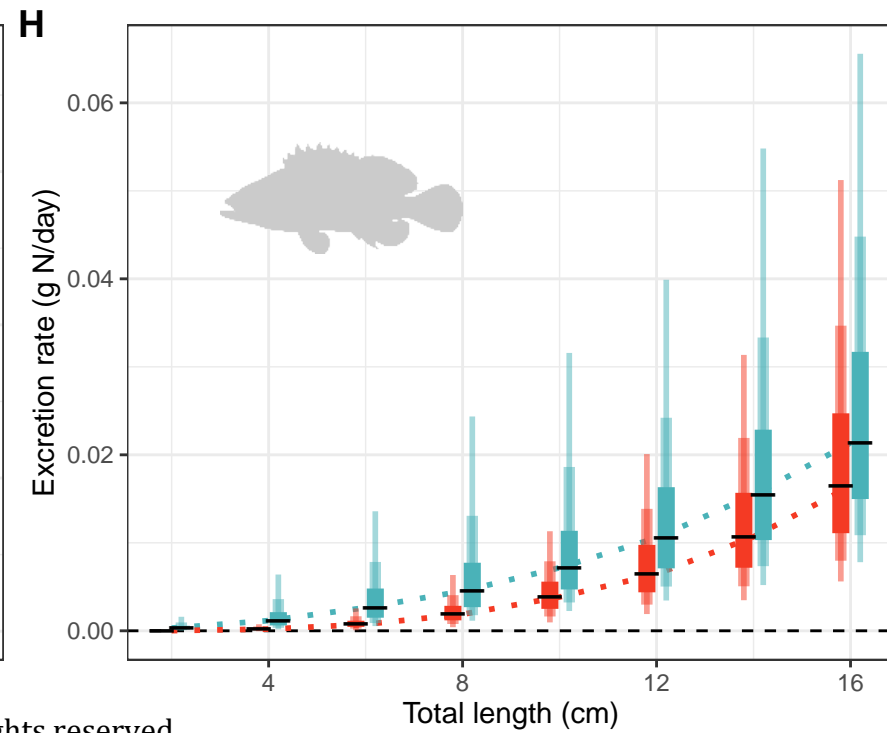
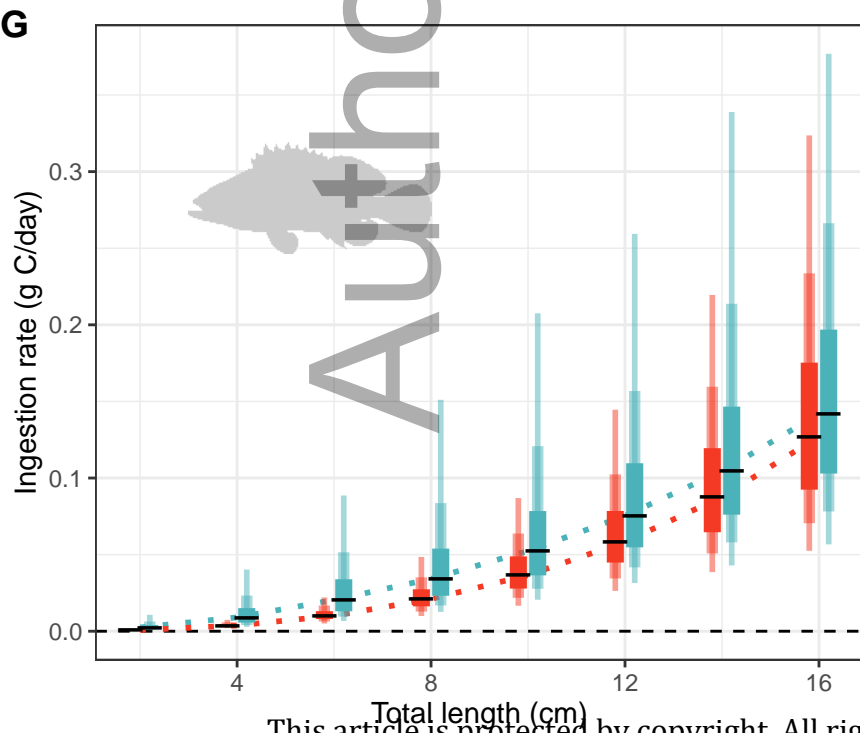
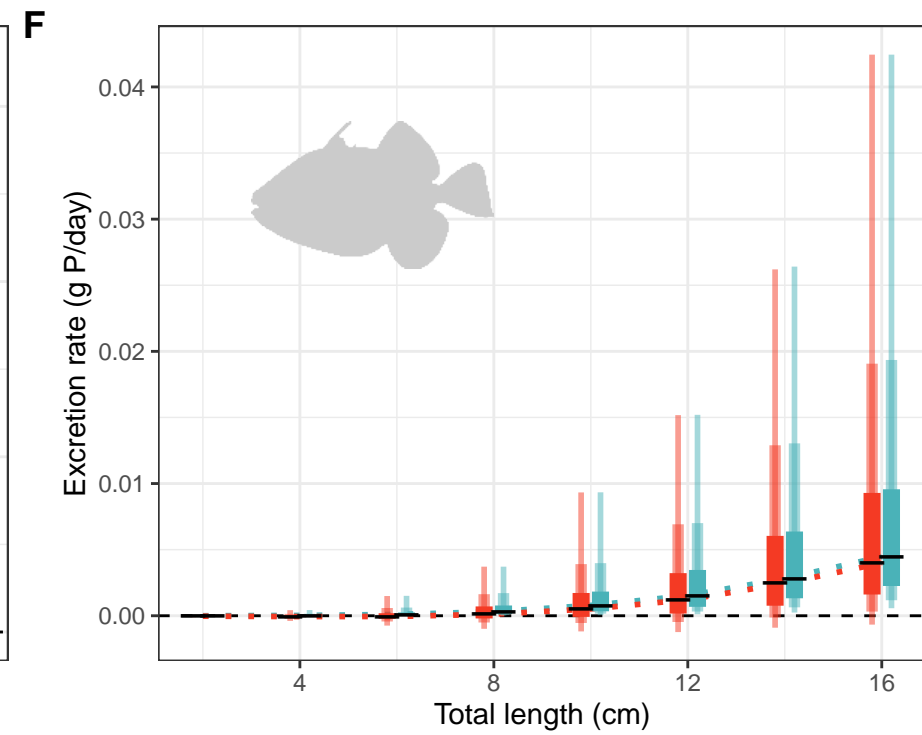
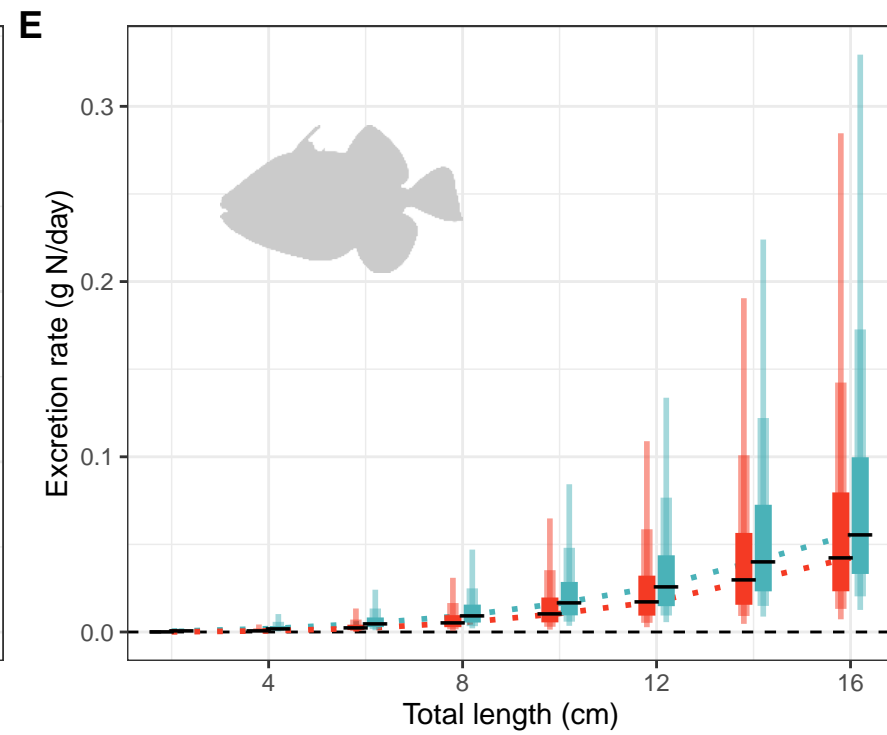
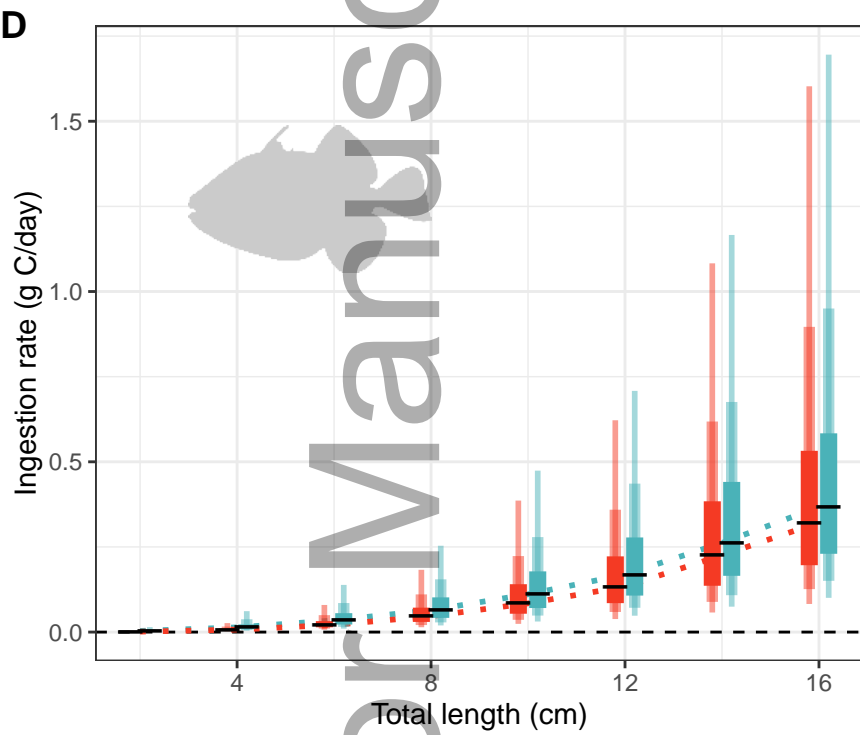
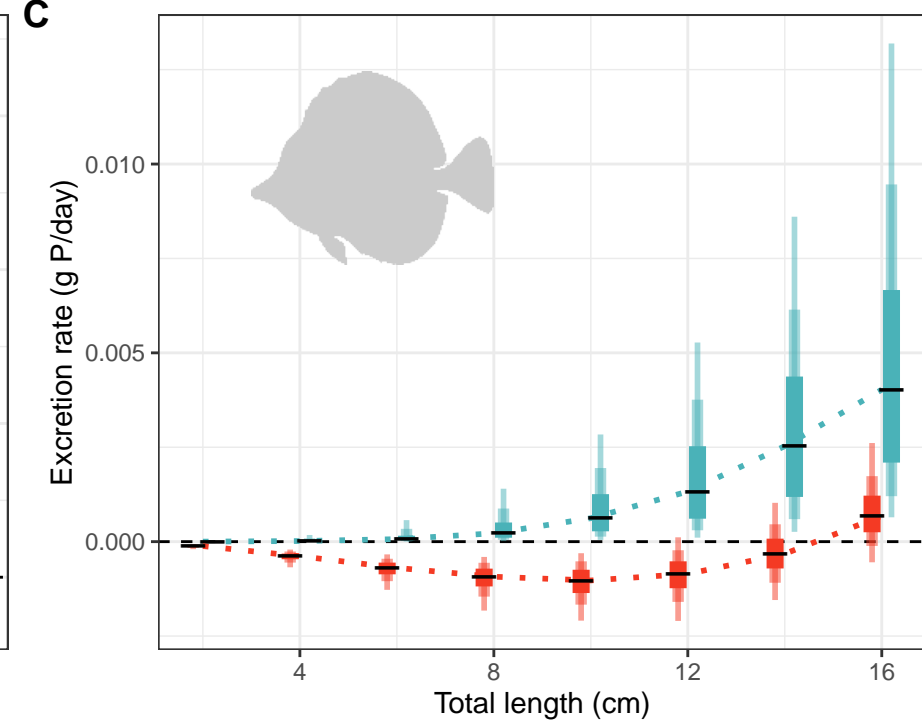
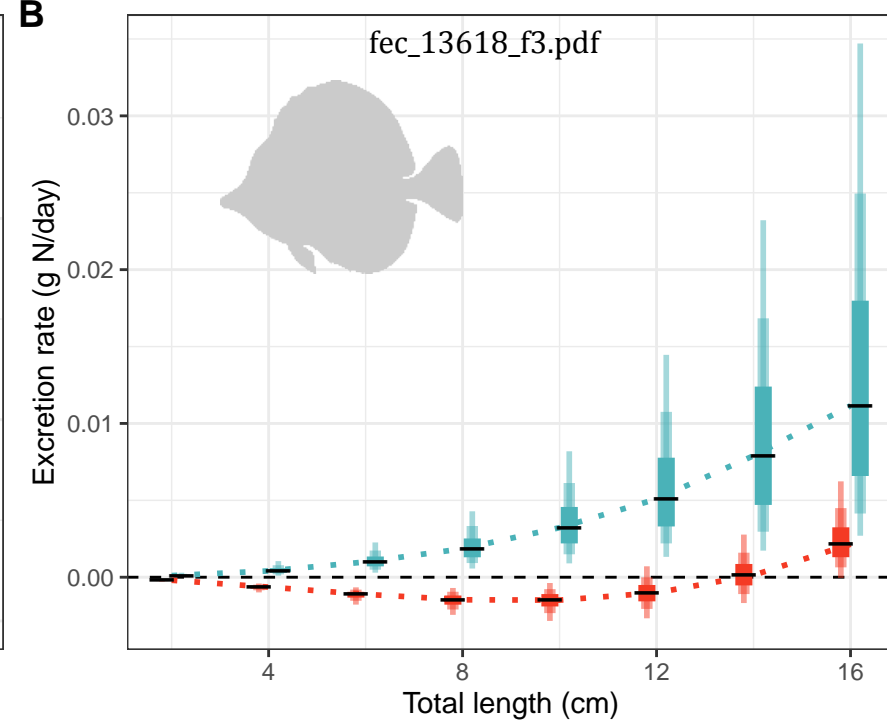
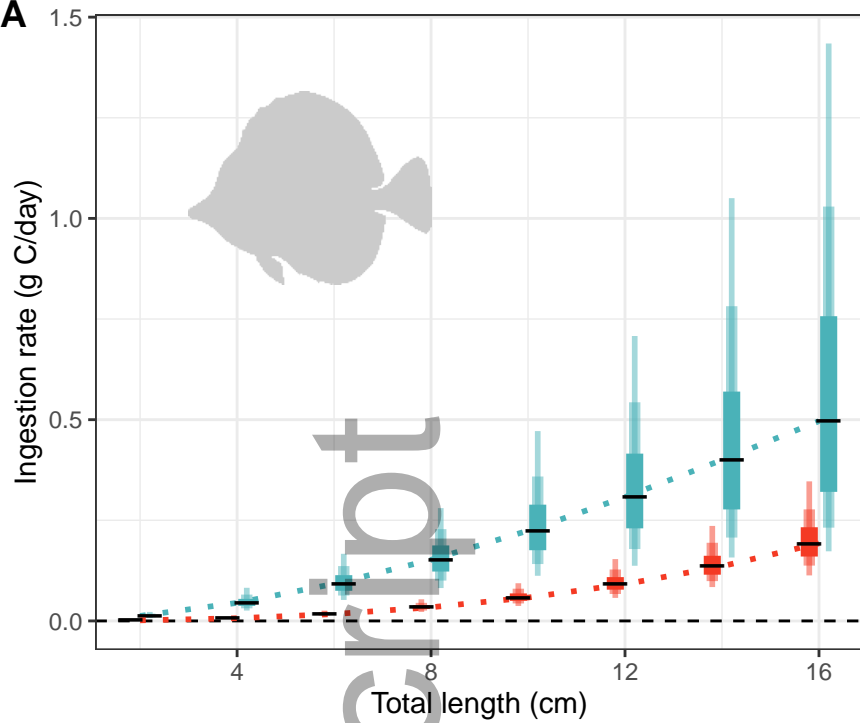


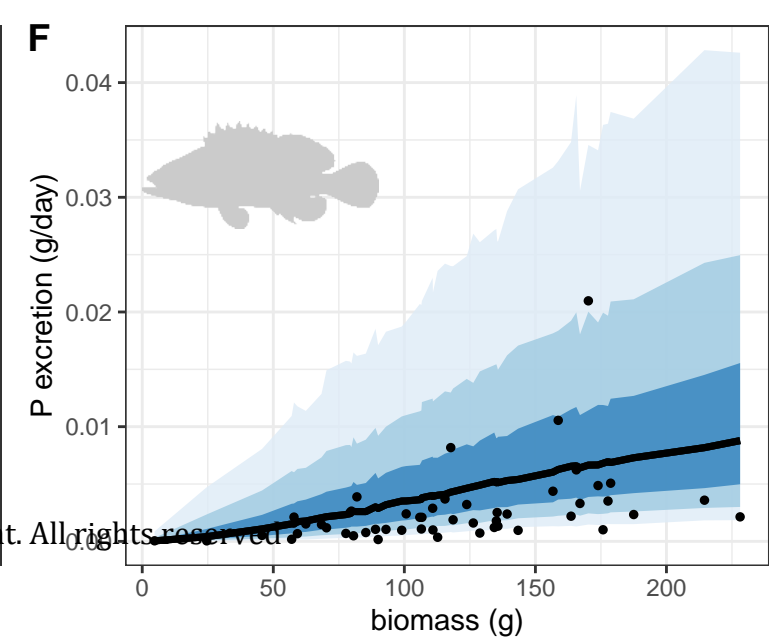
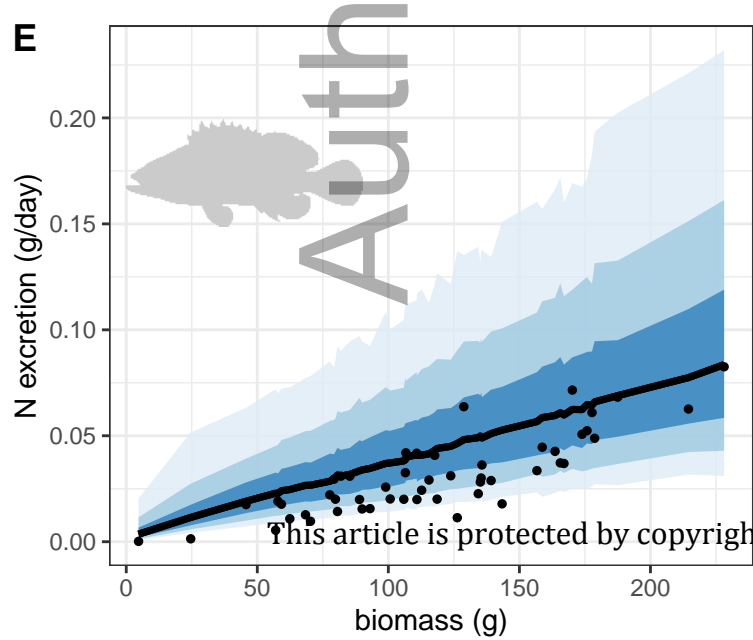
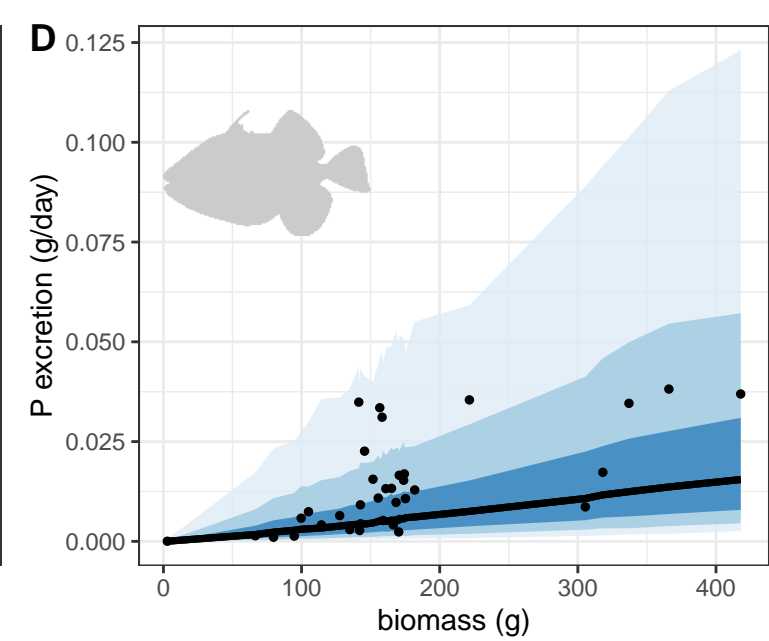
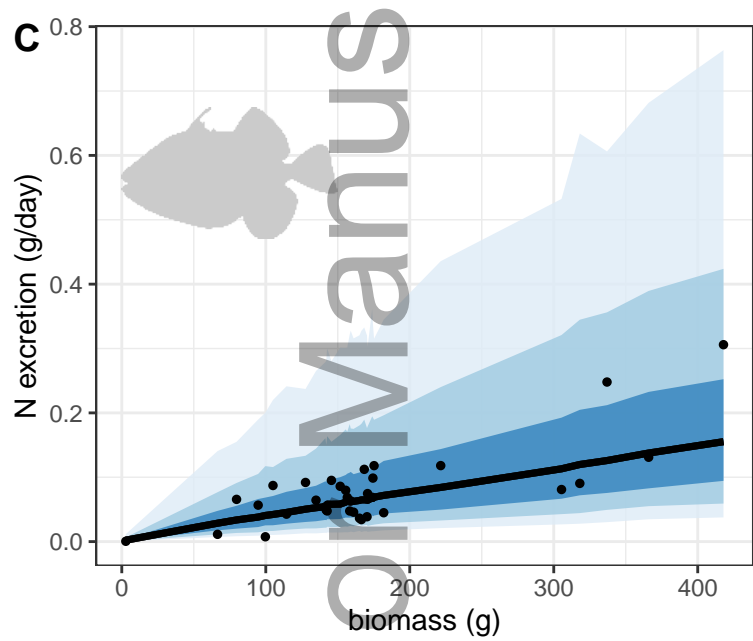
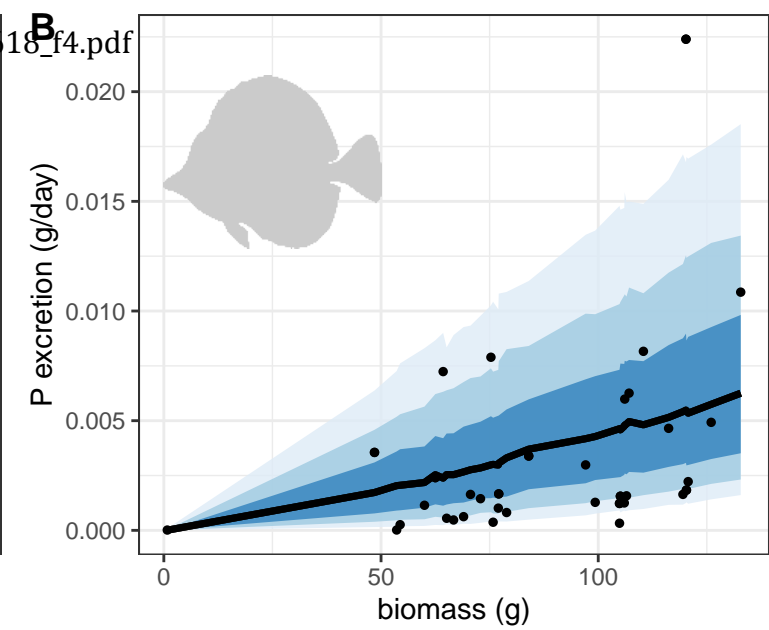
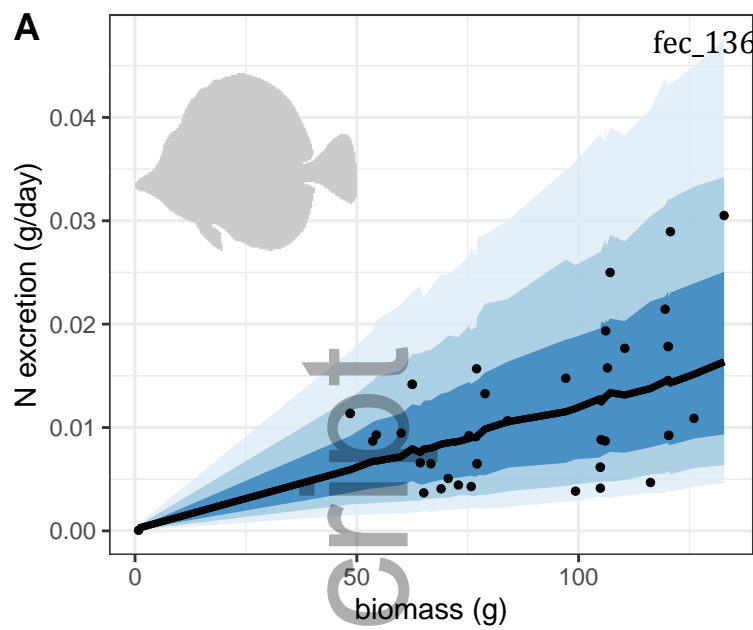
E. merra

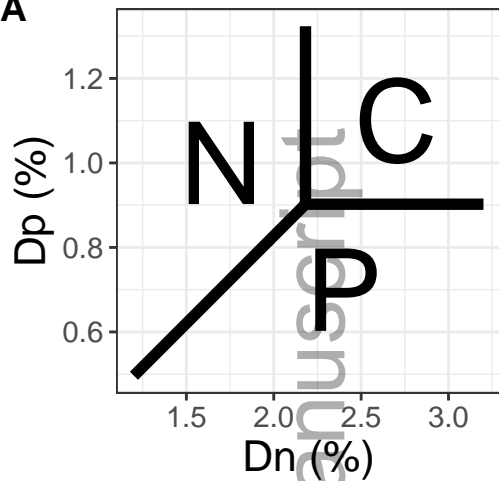
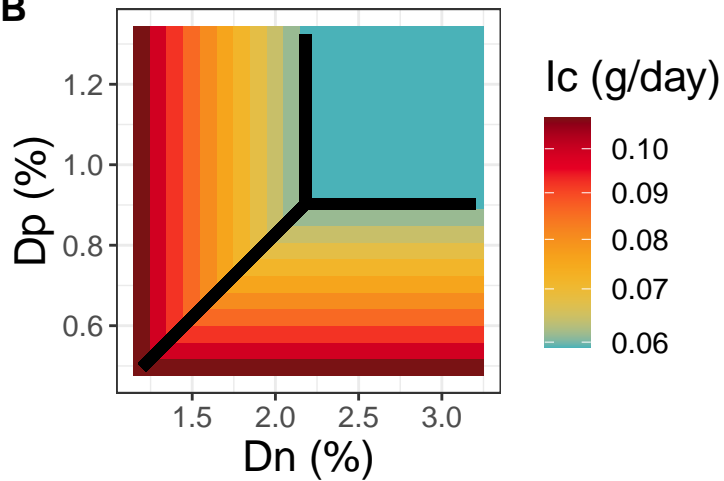
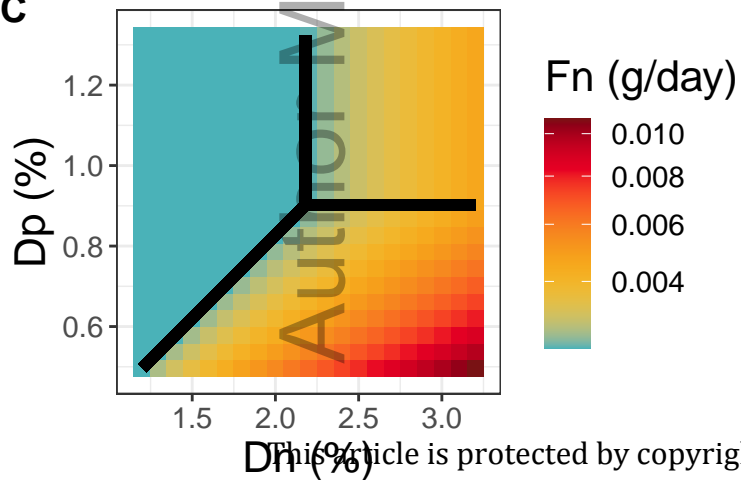


This article is protected by copyright. All rights reserved

Limiting element c n p





A**B****C****D**